

## GRENVILLIAN METAMORPHISM OF THE SUDBURY DIABASE DYKE-SWARM: FROM PROTOLITH TO TWO-PYROXENE – GARNET CORONITE\*

KATHRYN M. BETHUNE<sup>1</sup>

*Department of Geological Sciences, Queen's University, Kingston, Ontario K7L 3N6*

ANTHONY DAVIDSON<sup>1</sup>

*Geological Survey of Canada, 601 Booth Street, Ottawa, Ontario K1A 0E8*

### ABSTRACT

Coronite derived from olivine- and Fe–Ti-oxide-bearing diabase or gabbro is common in high-grade metamorphic terranes, but its progressive development from completely unmetamorphosed protolith has rarely been fully documented. Olivine diabase of the 1.24-Ga Sudbury continental dyke swarm, exposed across the Grenville Front southwest of Sudbury, Ontario, provides such documentation. Progressive textural and chemical changes are recorded by primary igneous and secondary metamorphic minerals, in rocks whose bulk chemistry has not changed, from unmetamorphosed diabase to coronitic metadiabase in which metamorphic conditions approached the granulite facies (>700°C at >8.0 kbar) during Grenvillian orogeny at ~1.0 Ga. Southeast-trending Sudbury dykes are undisturbed in the Southern and Superior province foreland of the Grenville orogen, but approaching the Grenville Front are offset by faults and locally contain greenschist-grade metamorphic assemblages. Deformed metadiabase dykes in the uplifted margin of the Grenville orogen, known from rock chemistry and U–Pb age of primary baddeleyite to be correlative with the Sudbury swarm, display reactions of both olivine and Fe–Ti oxide with plagioclase, leading to classic coronite development within a few kilometers of the front. Textural relationships indicate that peak metamorphism outlasted early deformation, compatible with a prograde P–T–t path. Of particular interest is comparison of the reactions between Fo<sub>70</sub> olivine and An<sub>60</sub> plagioclase (xenocrysts) and Fo<sub>35</sub> and An<sub>45</sub> (matrix) in the same rocks, and increase of Ti in biotite, Na and Al in clinopyroxene toward higher grade. Comparison of metamorphism in the dykes and their host rocks indicates telescoping of pre-Grenvillian isograds across the front.

*Keywords:* Sudbury diabase, Grenville Front, metamorphism, coronite, tectonic significance, Ontario.

### SOMMAIRE

La présence de coronite développée aux dépens de l'olivine et des oxydes de Fe–Ti est courante dans les diabases et les gabbros des socles à degré de métamorphisme élevé. En revanche, son développement progressif à partir d'une roche ignée non métamorphisée n'a été décrit que très rarement. Les filons de diabase à olivine de l'essai dit de Sudbury (1.24 Ga), affleurant de part et d'autre du front de Grenville au sud-ouest de Sudbury, Ontario, illustrent cette transition. Les changements progressifs en texture et en composition chimique sont enregistrés dans les minéraux primaires et les minéraux métamorphiques; les roches n'ont pas subi de changements dans leur composition globale dans la transition de diabase non métamorphisée à metadiabase coronitique, à des conditions dans le faciès granulite (>700°C, >8.0 kbar) au cours de l'orogénèse grenvillienne, à environ 1.0 Ga. Les filons, orientés vers le sud-ouest, ne sont pas perturbés dans les provinces dites Southern et Supérieure. Par contre, en approchant du front de Grenville, les filons sont déplacés le long de failles, et contiennent localement des assemblages du faciès schistes-verts. Les filons déformés de metadiabase dans la bordure du socle orogénique, reconnus à partir de la composition globale et de l'âge U–Pb de la baddeleyite primaire comme équivalents de l'essai de Sudbury, témoignent de réactions de l'olivine et des oxydes de Fe–Ti avec le plagioclase, ce qui a conduit au développement de coronite classique à quelques kilomètres du front. Les relations texturales montrent que les conditions de métamorphisme maximales ont perduré après les stades précoces de déformation, en conformité avec le tracé P–T–t prograde. D'intérêt particulier est la comparaison des produits de réaction dans les mêmes roches, impliquant l'olivine Fo<sub>70</sub> et le plagioclase An<sub>60</sub> d'origine xénocristique d'une part, et entre Fo<sub>35</sub> et An<sub>45</sub> de la matrice de l'autre. Aussi, il y a une augmentation en Ti dans la biotite, et en Na et Al dans le clinopyroxène, dans les roches les plus fortement affectées. Une comparaison du degré de métamorphisme des filons et de leurs roches-hôtes révèle une compression des isogrades pré-grenvilliens perpendiculaire au front.

(Traduit par la Rédaction)

*Mots-clés:* diabase de Sudbury, front de Grenville, métamorphisme, texture coronitique, signification tectonique, Ontario.

\* Geological Survey of Canada contribution number 1996481.

<sup>1</sup> *E-mail addresses:* bethune@geol.queensu.ca, tdavidson@gsc.nrcan.gc.ca

## INTRODUCTION

Metamorphosed mafic igneous rocks in high-grade terranes commonly display a corona structure (e.g., Shand 1945). Primary olivine and Fe–Ti oxide are surrounded by concentric zones of secondary minerals resulting from reaction with adjacent plagioclase. Non-aluminous secondary phases (orthopyroxene, clinopyroxene) are situated closest to olivine, whereas aluminous phases (garnet, biotite, pargasitic amphibole) occur next to plagioclase. Plagioclase is commonly clouded with submicroscopic spinel or corundum. Phase relations deduced from experimental petrology (e.g., Ringwood & Green 1966, Kushiro & Yoder 1966, Green & Ringwood 1967, Ito & Kennedy 1971, cf. Johnson & Essene 1982) suggest that such reactions occurred during passage from the stability field of olivine + anorthite into the fields of pyroxene–spinel and garnet granulite. The generally shallow positive slopes (P, ordinate; T, abscissa) of the reaction curves bounding these fields led some to propose that coronas formed during near-isobaric cooling following intrusion at depth (e.g., Griffin 1971, Griffin & Heier 1973, Emmett 1982, Grant 1987, 1988, Rivers & Mengel 1988). However, the role of magmatic interaction and the mechanism of reaction remain controversial. Whereas Joesten (1986) ascribed the formation of successive shells of the corona in troctolitic gabbro near Risør, Norway, to sequential, supersolidus (magmatic) reactions, most others (e.g., Whitney & McLelland 1973, Mongkoltip & Ashworth 1983, Ashworth 1986, Rivers & Mengel 1988, Grant 1988, Johnson & Carlson 1990) advocated the formation of coronas by simultaneous or sequential reactions in the subsolidus state. The consensus that the reactions are controlled by subsolidus processes involving diffusion has raised the alternative that, rather than forming during initial cooling, coronas may be produced during superimposed regional metamorphism (e.g., Mørk 1986, Johnson & Essene 1982, Johnson & Carlson 1990).

In this paper, we examine corona formation in dykes of olivine diabase of the Sudbury swarm (Fahrig *et al.* 1965, Fahrig & West 1986) where it is transected by the Grenville Front, the major tectonic boundary forming the northwestern margin of the Mesoproterozoic Grenville orogen. In the region southwest of Sudbury, Ontario (Fig. 1), this major continental swarm postdates early tectonic activity in the vicinity of the Grenville Front, but predates the Grenvillian orogeny (Palmer *et al.* 1977, Frarey 1985, Bethune & Davidson 1988, Bethune 1993, 1998). Undisturbed in the foreland, the dykes extend into the northwestern Grenville Province, where they cross-cut penetrative, front-parallel structures, are deformed, and show reaction of both primary olivine and Fe–Ti oxide with plagioclase, resulting in development of classic coronite within a few kilometers of the front.

In coronitic metadiabase southeast of the front, primary baddeleyite is surrounded or replaced by secondary zircon, inferred to have formed at the same time as the silicate coronas around olivine and Fe–Ti oxide in the same rock; the absence of coronas of either type in pristine Sudbury dykes northwest of the front provides a rationale for this interpretation. The zircon has been dated at ~1.0 Ga (Dudás *et al.* 1994), which is 240 million years younger than the age of crystallization of the swarm (~1.24 Ga; Krogh *et al.* 1987, Dudás *et al.* 1994), as dated by primary baddeleyite on both sides of the front. Age differences of comparable or greater magnitude between primary baddeleyite and secondary zircon in coronitic gabbro have been documented at other localities (e.g., 125 M.y.: Davidson & van Breemen 1988; 1060 M.y.: Tucker *et al.* 1990). Such age differences are considered too great for the secondary zircon (and by inference, related silicate coronas) to have formed during initial cooling, and instead point to an origin by superimposed (regional) metamorphism (cf. Johnson & Carlson 1990). Moreover, in the case of the Sudbury dyke swarm, the ~1.0-Ga age of secondary zircon corresponds closely to ages obtained for Grenvillian metamorphism from other rocks in the region (Haggart *et al.* 1993, Krogh 1994), which can reasonably be interpreted to result from crustal thickening brought about by thrust deformation along the northwestern margin of the Grenville Province near the end of the Grenvillian orogenic cycle (1.3–1.0 Ga: Moore 1986; cf. Davidson 1995). The Sudbury dykes thus afford a rare opportunity to document the progressive development of coronas from a wholly unmetamorphosed protolith in a prograde setting.

## REGIONAL SETTING AND AGE RELATIONSHIPS

Between Killarney and Sudbury, Ontario (Fig. 1), the Grenville Front is a zone of faulting and mylonitization separating domains of contrasting structural style. In the Southern Province foreland, supracrustal rocks of the Huronian Supergroup ( $\leq 2.45$  Ga: Krogh *et al.* 1984) intruded by Nipissing gabbro sills (2.22 Ga: Corfu & Andrews 1986, Noble & Lightfoot 1992) are folded about east-trending axes and metamorphosed mainly to the greenschist facies, effects ascribed to the Penokean orogeny (1.89–1.83 Ga: Bickford *et al.* 1986). Close to the Grenville Front, Penokean structures are truncated by several northeast-elongate, late Paleoproterozoic and early Mesoproterozoic granite plutons (~1.74 and ~1.47 Ga: van Breemen & Davidson 1988, Davidson & van Breemen 1994). Granites of both ages and their Huronian country rocks are characterized by subvertical to southeast-dipping foliation, likely of composite age, and are also cut by a number of discrete, steep, northeast-striking faults. Southeastward, foliation within these rocks intensifies toward a prominent, southeast-dipping zone of mylonite and

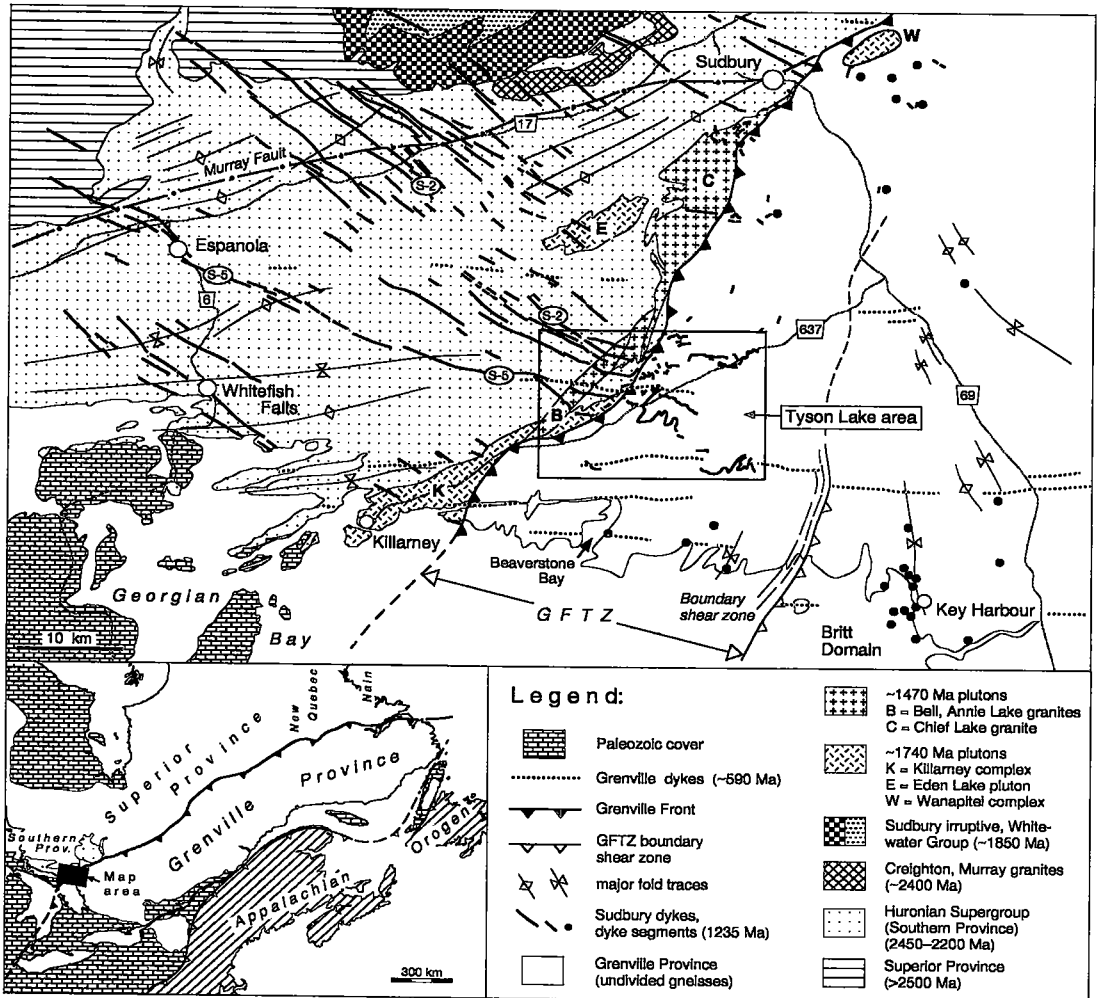


FIG. 1. Geology of the region southwest of Sudbury, Ontario (modified after Card & Lumbers 1977, Card 1978) showing the extent of the Sudbury diabase dyke-swarm in the Southern Province and correlative dykes of metadiabase in the Grenville Province.

ultramylonite that carries kinematic evidence for northwest-directed, thrust-sense displacement, and marks an abrupt southeastward increase (up-section) in metamorphic grade. In the hanging wall of this zone, a 10–20-km-wide belt of upper amphibolite- to granulite-facies gneiss with structures of similar style and orientation is known as the Grenville Front tectonic zone (GFTZ; Wynne-Edwards 1972). Metaplutonic rocks in the GFTZ have the same primary igneous ages as the plutonic rocks in the foreland (e.g., ~1.7 Ga, 1.45 Ga; Davidson *et al.* 1992); however, because of the intense strain and high grade of metamorphism, it is uncertain whether associated supracrustal schist and gneiss are correlative with the Huronian Supergroup

(Frarey 1985, Bethune & Davidson 1988). A major high-strain zone delineates the southeastern boundary of the GFTZ, beyond which the structural style changes to broad, open folds with shallowly southeast-plunging axes characteristic of the Britt domain (Culshaw *et al.* 1983, 1988; Fig. 1).

#### *Sudbury dykes as tectonic markers*

The Killarney–Sudbury segment of the front has long been suspected to have a protracted history of northwest-directed thrust uplift, extending possibly as far back as early Paleoproterozoic time and culminating with the Grenvillian orogeny at ~1.0 Ga (e.g. Krogh &

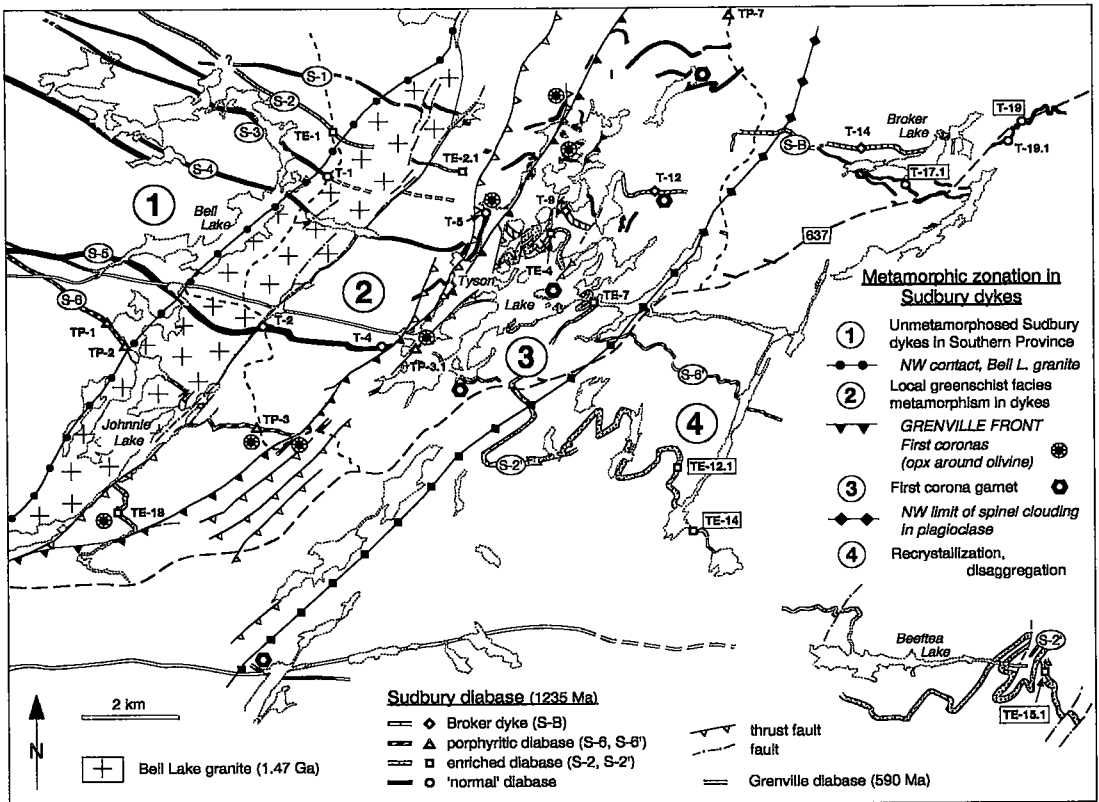


FIG. 2. Metamorphic zonation exhibited by the Sudbury dykes across the Grenville Front in the Tyson Lake area. Sample locations selected for mineral chemistry and thermobarometry are numbered (T, normal diabase; TP, porphyritic diabase; TE, Fe-enriched diabase; see Tables 1, 2, and text) and are the same as in Bethune (1993).

Davis 1970, Brocoum & Dalziel 1974, Lumbers 1975, 1978; cf. Davidson 1990). However, deciphering this history has proven difficult, mainly because Grenvillian and pre-Grenvillian structures along and southeast of the front have similar orientations. The Sudbury dyke swarm (1.24 Ga), which represents the youngest pre-Grenvillian geological unit in the region, is a critical marker for resolving different generations of structures and related metamorphism. Northwest of the Grenville Front, southeast-striking dykes of the swarm are vertical, range from a few meters to as much as 100 m thick, and strike uniformly southeast, cutting the east-west folds in the Southern Province. Approaching the Grenville Province, the dykes cut the northeast-trending foliation in the Huronian Supergroup and in Paleo- and Mesoproterozoic granite (Card & Lumbers 1977, Card 1978, Fahrig & West 1986), but are themselves cut by the steep faults with minor lateral offset. Farther southeast, the dykes are abruptly truncated by the prominent zone of mylonite, approaching which their trends become less regular. In the GFTZ to the southeast, the correlative dykes are deformed and

metamorphosed, but maintain a cross-cutting relationship to pre-existing gneissic layering.

The dykes thus reveal a pronounced difference in pre-Grenvillian structural style and metamorphism across the front; in particular, they demonstrate that much of the structural grain in the GFTZ is pre-Grenvillian (Bethune 1998). The high-grade metamorphism that accompanied the deformation responsible for this trend and, by inference, the pre-dyke deformation along the Grenville Front, has been dated by the U-Pb method on zircon, monazite and titanite (respectively, Krogh 1994, Dudás *et al.* 1994, Haggart *et al.* 1993) at ~1.45 Ga, indicating that it was broadly coeval with Mesoproterozoic plutonism in the region. The steep pre-dyke foliation in the Paleo- and Mesoproterozoic plutons immediately northwest of the front is presumed to be in part related to this deformation (*i.e.*, ~1.45 Ga; Bethune 1993). It is notable, however, that field relationships in the GFTZ (*e.g.*, Davidson & Bethune 1988) point to an even older tectonic history for the country rocks of Mesoproterozoic plutons. The Sudbury dykes thus appear to have

intruded across an older (~1.45 Ga) structural front and, some 240 M.y. later, were deformed and metamorphosed during the Grenvillian orogeny. The Grenville Front can be clearly defined as a 3–4-km-wide zone wherein the dykes are disrupted by high-level brittle faults and, farther southeast, are truncated abruptly by the major mylonite zone. The progressive metamorphism of the dykes across this zone is well illustrated in the Tyson Lake area (Fig. 1), where these relationships have been studied in detail (Bethune & Davidson 1988, Bethune 1989, 1993, 1997).

#### THE TYSON LAKE AREA

One of the highest concentrations of Sudbury diabase dykes at the southeast margin of the Southern Province is at Tyson Lake, roughly halfway between Killarney and Sudbury (Fig. 1), where six major dykes are intersected by the Grenville Front (Fig. 2). From northwest to southeast across the Tyson Lake area, the dykes show a systematic increase in metamorphic grade and a change in style of deformation in concert with their host rocks, allowing definition of four structural and metamorphic zones. Zone 1 encompasses the area northwest of the 1.47-Ga Bell Lake granite, where unmetamorphosed dykes cut tightly folded greenschist-facies rocks of the Huronian Supergroup. In Zone 2, which extends from the northwestern contact of the Bell Lake granite to Tyson Lake, the dykes maintain their southeastward course; they cut the steep to moderately southeast-dipping foliation in all rock units, but are themselves cut by steep, brittle faults, along which they are strongly sheared and contain greenschist-facies assemblages. Approaching Tyson Lake in Zone 2, several dykes show a pronounced northeastward deflection in strike, and all are truncated by the major zone of mylonite in the southeastern part of the Grenville Front zone. Southeast of this zone of mylonite, which forms the northwestern boundary of Zone 3, dykes cutting upper amphibolite-(K-feldspar – sillimanite zone) to granulite-facies gneiss (locally containing orthopyroxene – garnet – sillimanite), have irregular map patterns and are internally strained (Frarey 1985, Bethune 1993). The onset of irregular geometry in the swarm at the mylonite zone is interpreted to be the result of a combination of irregular primary intrusion and superimposed deformation by buckle folding (Bethune 1998). Within a few hundred meters northwest of the same mylonite zone, the dykes show the first signs of metamorphism, expressed by the appearance of narrow coronas of orthopyroxene around olivine, and growth of secondary biotite around Fe–Ti oxide. Southeastward, coronas show a progressively greater degree of development, in some cases with production of an outer garnet–pyroxene symplectite. Concomitantly, plagioclase in the rock becomes increasingly clouded by submicroscopic spinel (*cf.* McLelland & Whitney

1980). The northwestern boundary of Zone 4 is placed at the northwestern limit of noticeably darkened cores of plagioclase laths, between 3 and 5 km southeast of the front.

The gradual and continuous development of dyke metamorphism across the Zone 2 – Zone 3 boundary contrasts strongly with the abrupt increase in host-rock metamorphic grade, suggesting that relative (thrust-sense) displacement had already taken place along or close to the front before dyke emplacement, and hence also before Grenvillian orogeny (*cf.* Haggart *et al.* 1993). Preserved chilled margins of dykes in Zone 3 cut across metamorphic minerals in their host rocks (Bethune 1993), attesting to the existence of pre-dyke high-grade metamorphism, subsequently dated at ~1.45 Ga (U–Pb monazite: Dudás *et al.* 1994). Following tectonism at ~1.45 Ga, rocks in the vicinity of the front must have been uplifted and eroded before intrusion of the 1.24-Ga Sudbury swarm of continental diabase dykes, which is assumed to have been emplaced in a quiescent tectonic environment.

#### *Geochemical correlation and distinctive dykes*

Correlation of the Sudbury swarm across the Grenville Front in the vicinity of Tyson Lake was first proposed by Palmer *et al.* (1977) on the basis that Sudbury diabase has a distinctive alkaline composition that sets it apart from most other swarms in the Canadian Shield (Fahrig *et al.* 1965, Condie *et al.* 1987). In order to verify this correlation, which the previously reported geochronological correlation has corroborated, the Sudbury diabase in the Southern Province (Zones 1 and 2) and metadiabase dykes in the Grenville Front tectonic zone (Zones 3 and 4) were sampled extensively. An example of the results of this geochemical survey, reported in detail in Bethune (1993), is presented in Figure 3. Trace-element plots normalized to mid-ocean-ridge basalt (MORB) demonstrate that metadiabase in the Grenville Province is compositionally indistinguishable from Sudbury diabase northwest of the Grenville Front; both are olivine normative and have characteristically high abundances of Fe, K, Ba, Ti, P, Zr and the light rare-earth elements (*LREE*). There are no appreciable differences in content of alkalis or volatile components, such as might be expected had the metadiabase been subjected to infiltration of fluid during metamorphism. Thus the mineralogical differences exhibited by the change from primary igneous assemblages in the Grenville foreland to metamorphic assemblages in the GFTZ can be considered to have developed without appreciable addition or loss of chemical components, *i.e.*, within a closed chemical system. Figure 3 also highlights the distinctive chemical signature of Sudbury diabase relative to diabase of the much younger Grenville swarm (~590 Ma; Kamo *et al.* 1995), whose dykes cut the Grenville Front without disturbance in the same area (Figs. 1, 2).

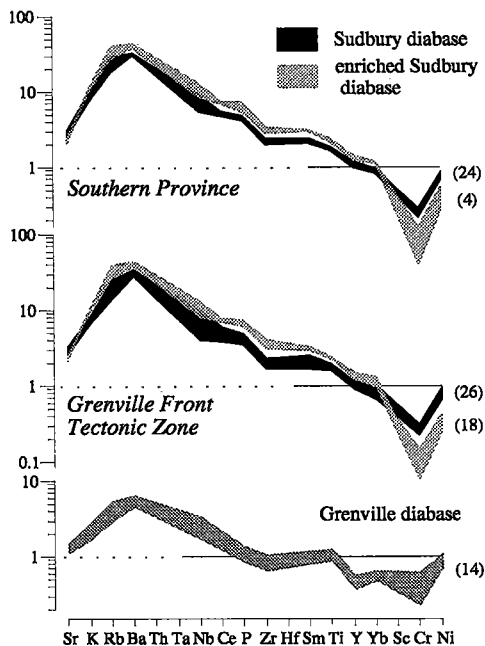


FIG. 3. MORB-normalized spidergrams (Pearce 1983) comparing Sudbury diabase in the Southern Province, metadiabase in the Grenville Front tectonic zone, and post-tectonic diabase of the Grenville swarm. Upper and lower limits are  $\pm 1\sigma$ ; numbers in parentheses indicate number of compositions averaged.

Another important result of the geochemical survey is recognition that the Sudbury swarm has a bimodal character, exemplified principally by one dyke (S2) that contains greater than average abundances of Fe, K, Ba, Ti, P and LREE relative to diabase from other dykes in the swarm, whose average composition is defined as "normal" (Fig. 3; Bethune 1993). Certain other dykes display a more restricted compositional range within the "normal" field. These chemical differences, along with a number of field and petrographic traits, permit correlation of individual dykes across the Grenville Front. Dyke S-2 is correlated with a dyke in the GFTZ showing identical Fe and incompatible element enrichment (S-2'); the latter dyke can be traced discontinuously along a sinuous course for 18 km into the Grenville Province (Figs. 1, 2). Another dyke northwest of the front, S-6, is characterized by large phenocrysts of plagioclase along its margins. Southeast of the front, this dyke is compositionally matched with a thinner porphyritic dyke and correlative offshoots (Figs. 1, 2; Bethune 1993). Another potential correlation is made

between four thick segments of dyke that strike east-southeast between Tyson and Broker lakes. Compositions of metadiabase from these four segments, identified as S-B ("Broker dyke") in Figure 2, allow correlation on the basis that they are the least fractionated (*e.g.*, greatest CaO, Mg#) among the "normal" diabase population. This dyke is chemically similar to a dyke of comparable thickness northwest of the front (S-5).

In summary, identification and mapping of chemically distinct dykes across the Grenville Front in the Tyson Lake area have facilitated comparison of progressive metamorphism between contrasting bulk-compositions in what can reasonably be inferred from the analytical study to have been a closed chemical system.

#### PETROGRAPHY

The following petrographic descriptions trace the changes observed in Sudbury diabase and metadiabase across the zones outlined above; these changes are illustrated schematically in Figures 4 and 5.

#### Nature of the protolith, Zone 1

Fresh Sudbury diabase in Zone 1 is typically fine to medium grained, with a subophitic texture (Fig. 4A). Primary minerals, in order of relative abundance, are plagioclase, augite, olivine and Fe-Ti oxide, the latter being a finely exsolved solid-solution between magnetite and ulvöspinel containing lamellae of ilmenite. Accessory minerals are apatite, biotite and K-feldspar; baddeleyite and sulfides (pyrite, pyrrhotite, chalcopyrite) are present in trace amounts. Biotite occurs as single crystals associated with Fe-Ti oxide; K-feldspar is found in interstices between plagioclase laths and is variably perthitic. The texture of Fe-enriched diabase from dyke S-2 does not differ from that of normal, nonporphyritic diabase; however, consistent with the normative differences between the two types, Fe-enriched diabase generally has a higher color index and contains more apatite and K-feldspar.

The porphyritic variety of diabase is characterized by large ( $\leq 4$  cm) blocky phenocrysts of plagioclase in a matrix of fine-grained diabase that is identical in mineralogy and texture to nonporphyritic diabase. The plagioclase phenocrysts show no optical evidence of zoning except at their margin, where a narrow rim has a more sodic composition. The large, uniformly calcic core of these phenocrysts has rounded edges, indicative of resorption. Olivine crystals  $\leq 5$  mm in diameter are included within (Fig. 5A), or lie along the margins of, plagioclase phenocrysts; more rarely, they occur as isolated phenocrysts up to 1 cm in diameter. These features, along with the fact that the phenocrysts and included olivine are more primitive in composition than plagioclase and olivine in the matrix (suggested

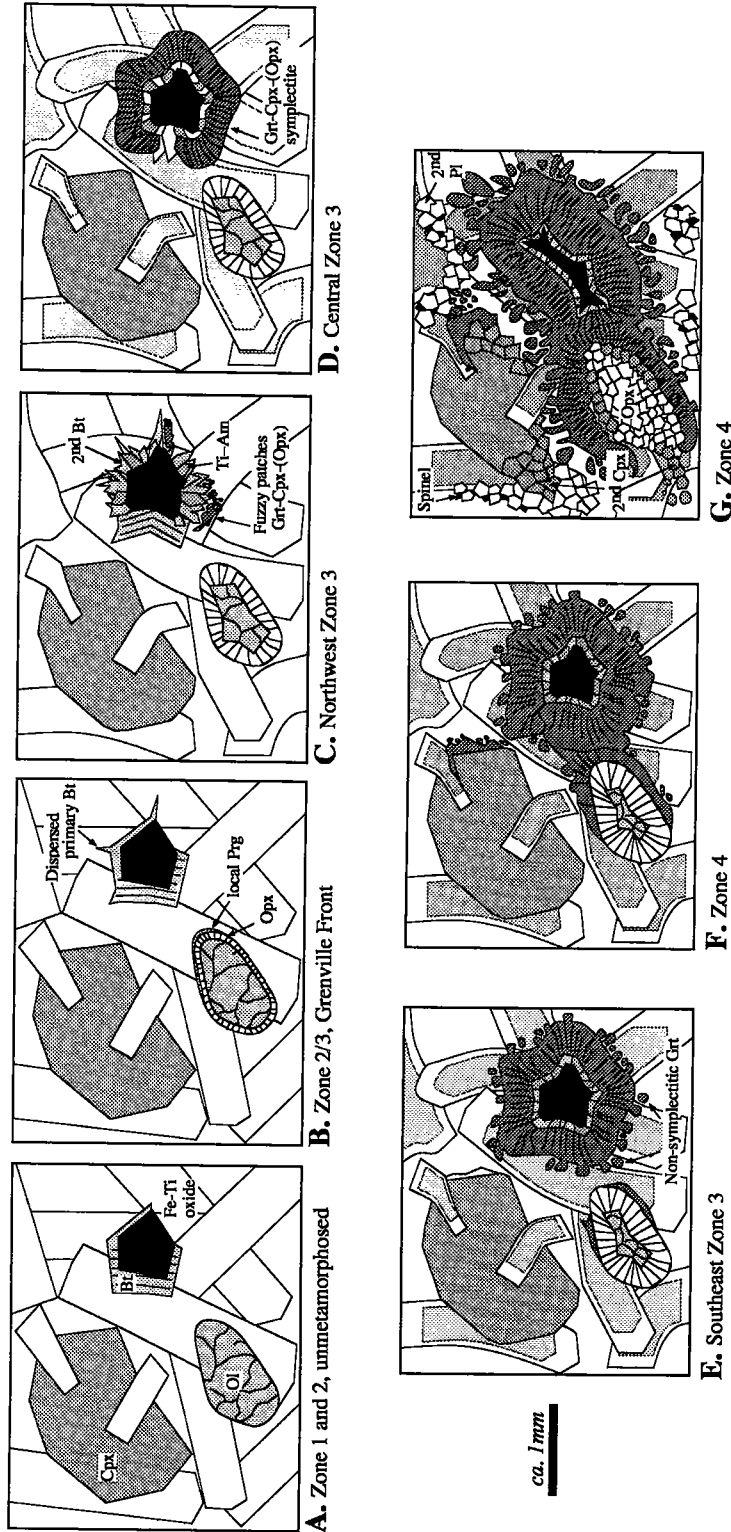


FIG. 4. Progressive development of coronas around olivine and Fe-Ti oxide in Sudbury diabase. Sketches represent typical textural relations observed in thin section. A. Unmetamorphosed olivine diabase typical of Sudbury dykes of Zone 1, and of undisturbed parts of dykes in Zone 2. B. Onset of corona-forming reactions at the Grenville Front. Narrow rim of orthopyroxene surrounds olivine. Primary biotite is partly recrystallized and dispersed. C. Orthopyroxene rims are wider in northwestern Zone 3. Secondary biotite and olive-green titanian amphibole have partly overgrown primary biotite. Fuzzy patches representing initial growth of Grt-Cpx-(Opx) symplectite have nucleated in plagioclase beside Fe-Ti oxide coronas. D. Grt-Px symplectite forms a well-defined rim. The core of plagioclase laths show first the faint but noticeable clouding by spinel. E. Grt-Px symplectite rim is wider in southeastern Zone 3, embaying plagioclase. Outermost garnet lacks pyroxene inclusions. F. Grt-Px symplectite in Zone 4 is evident around olivine coronas and locally along the interfaces between plagioclase and other primary minerals. The core zone of plagioclase grains is more strongly clouded. G. Grt-Px symplectite fully encircles both Fe-Ti oxide and olivine, which are strongly embayed. The olivine "core" has been replaced by a mosaic of fine orthopyroxene. Garnet has encroached farther into plagioclase, which has locally recrystallized, exsolving discrete grains of spinel.

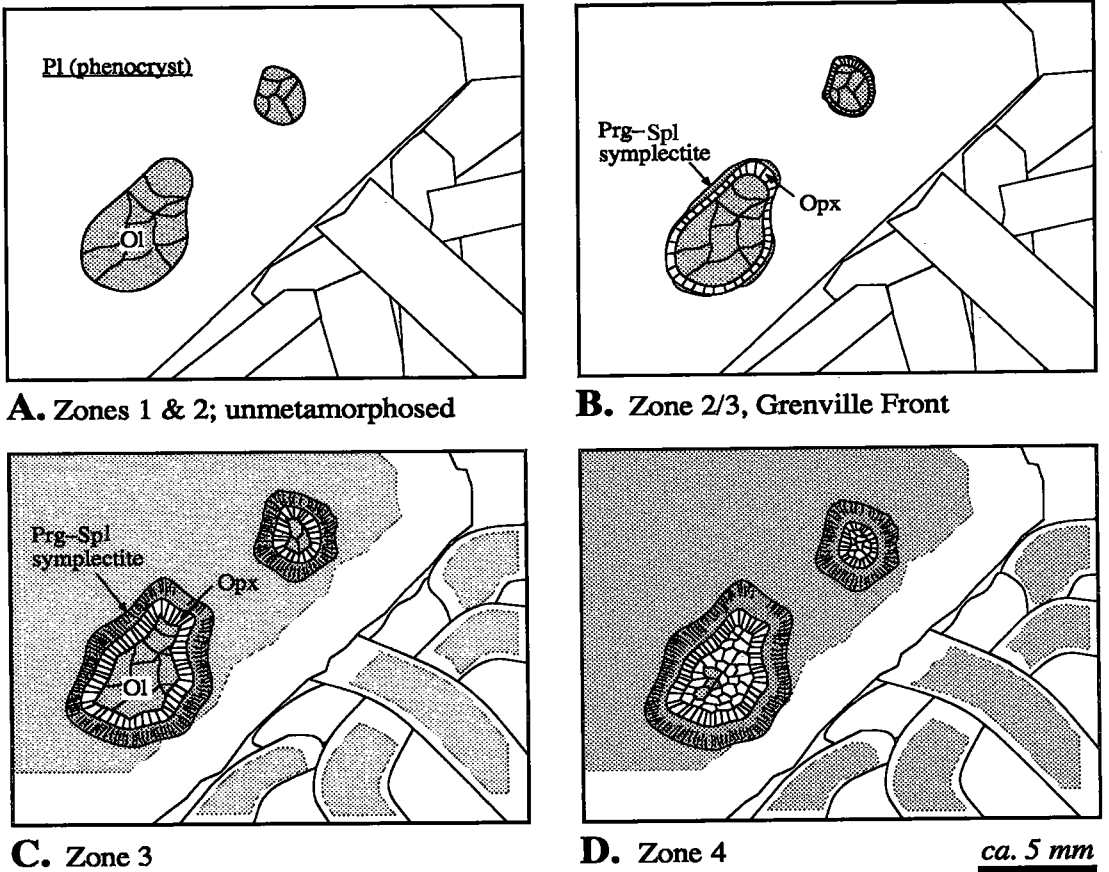


FIG. 5. Progressive development of coronas around olivine in plagioclase xenocrysts of porphyritic Sudbury diabase. A. Olivine inclusions in plagioclase xenocrysts in Zones 1 and 2 show no sign of reaction. B. At the Grenville Front, olivine is mantled by successive thin rims of orthopyroxene and symplectically intergrown pargasite and spinel. C. Orthopyroxene and Prg-Spl coronas in Zone 3 have widened at the expense of olivine; plagioclase shows first signs of clouding by submicroscopic spinel. D. Olivine in Zone 4 has been almost fully replaced by orthopyroxene, and spinel clouding in plagioclase has intensified.

by optical properties and confirmed by results of electron-microprobe analyses; below), suggest that the phenocrysts should be considered.

#### *Greenschist-facies assemblages, Zone 2*

In Zone 2, diabase shows no sign of metamorphic reaction except near faults, where sheared metadiabase typically contains chlorite, actinolite and epidote. Along the faulted southeastern contact of the Bell Lake granite, plagioclase xenocrysts in dyke S-6 are clouded, rather than clear, resulting from growth of fine-grained subgreenschist- to greenschist-facies minerals (e.g., prehnite, epidote). Olivine in the xenocrysts is variably replaced by carbonate, serpentine, chlorite, and cummingtonite. Growth of these mineral

assemblages under greenschist-facies conditions was thus strongly controlled by the availability of fluid.

#### *Development of coronas, Zones 3 and 4*

Starting at the boundary between Zones 2 and 3, and concomitant with the onset of penetrative deformation of primary minerals (notably plagioclase), the Sudbury diabase shows a progressive increase southeastward through Zones 3 and 4 in the production of metamorphic minerals as coronas around olivine and Fe-Ti oxide in contact with plagioclase. The first appearance of coronas at the Grenville Front is marked by the occurrence of a narrow rim of orthopyroxene around olivine and recrystallization and dispersion of primary biotite in the vicinity of Fe-Ti oxide (Figs. 4B

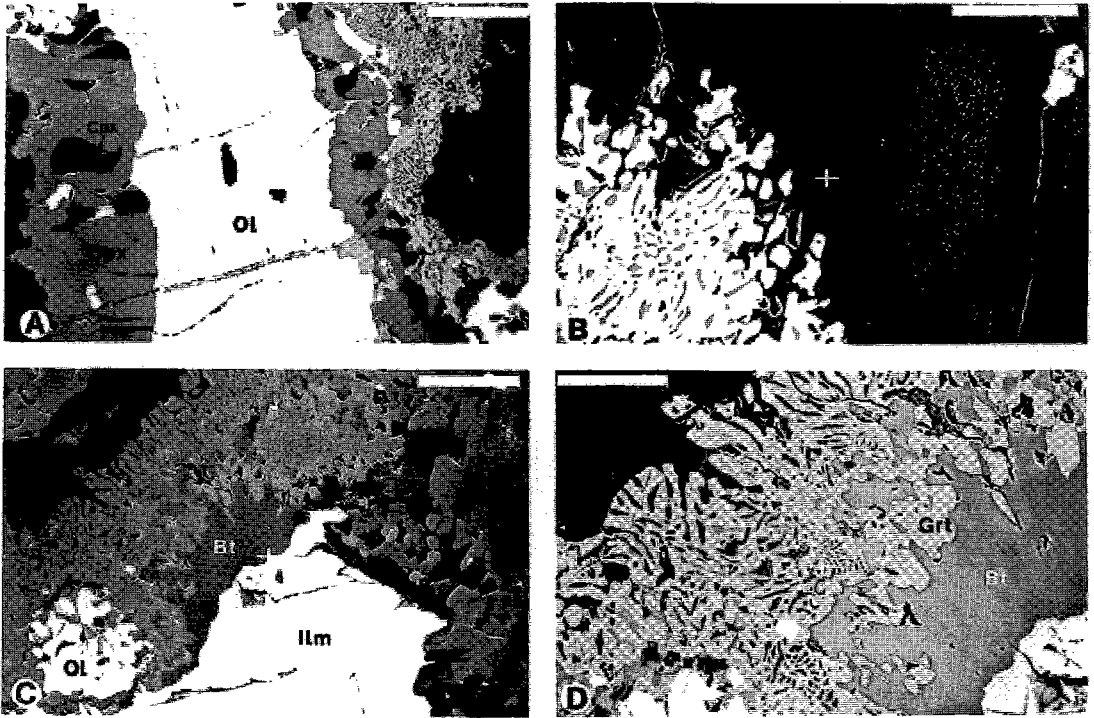


FIG. 6. Scanning electron photomicrographs of corona textures (sample TE-12.1). A. Asymmetrical olivine corona – olivine core is surrounded by orthopyroxene layer containing several equant to tapered grains of secondary clinopyroxene; a thin Grt-Px symplectite rim is discontinuously developed on right-hand side of corona only. Equivalent to stage depicted in Figures 4E and F (scale bar 100  $\mu$ m). B. Close-up of margin of Grt-Px symplectite. Note that the outermost garnet has lost pyroxene inclusions; the pyroxene occurs as discrete grains. K-feldspar (lighter in color than plagioclase) is intergrown with the outermost garnet. The core of an adjacent lath of plagioclase is outlined by the high reflectivity of included grains of spinel (scale bar 50  $\mu$ m). C. Ilmenite and olivine cores share a common outer rim of Grt-Cpx-(Opx) symplectite, which corresponds to a more advanced stage of development of symplectite than that shown in A (scale bar 100  $\mu$ m). D. Close-up of the Grt-Px symplectite shown in C (scale bar 50  $\mu$ m).

and 5B). In some places, the orthopyroxene coronas are surrounded by a discontinuous rim of pale green amphibole. Southeastward within Zone 3, this amphibole disappears from coronas around matrix olivine as orthopyroxene coronas become wider and olivine cores decrease in size and are progressively embayed (Fig. 4C). Olivine enclosed in plagioclase xenocrysts, on the other hand, has enlarged coronas consisting of an inner rim of orthopyroxene and an outer one of pale green amphibole symplectitically intergrown with dark green spinel (Fig. 5C). Although not a participant in corona-forming reactions, primary augite is noticeably darker in Zone 3 than northwest of the front, owing to exsolution of ilmenite as fine, closely spaced lamellae. Primary biotite in the vicinity of oxide grains is locally completely overgrown by secondary biotite, itself irregularly intergrown with olive-green amphibole (Fig. 4C). At this stage, extremely fine-grained material with high relief is

commonly seen within plagioclase close to biotite or amphibole of oxide coronas (Fig. 4C). Scanning electron microscopy reveals that these "fuzzy patches" represent the initial stages of growth of garnet – clinopyroxene – (orthopyroxene) symplectite. Garnet symplectite occurs more copiously and closer to the front in dyke S-2' than in any of the other dykes. These patches of symplectite enlarge and coalesce to form continuous outer rims in central Zone 3, where laths of primary plagioclase show the first obvious clouding related to the formation of spinel (Fig. 4D).

Toward and within Zone 4, garnet-pyroxene symplectite is increasingly evident in the outer part of coronas around matrix olivine, as well as along interfaces between plagioclase and other primary minerals (Figs. 4E, 4F, 6A); spinel clouding in plagioclase becomes more intense (Fig. 6B). At their full development (Fig. 4G), coronas in Zone 4 are typically elongate with ragged, "dispersed" edges.

TABLE 1. AVERAGE COMPOSITIONS OF PRIMARY AND METAMORPHIC FERROMAGNESIAN MINERALS IN SUDBURY DIABASE AND METADIABASE.

Sample no.	Zone 1					Zone 2					Zone 3					Zone 4				
	TP-1	TE-1	T-1	T-2	TE-1	TP-3	TE-18	T-4	T-5	TE-4	T-9	T-12	TE-7	T-14	<u>TE-12.1</u>	<u>T-17.1</u>	<u>TE-14</u>	<u>T-19</u>	<u>TE-15.1</u>	
Mg# (rock)	40	32	43	39	-	40	32	40	41	34	48	44	35	44	-	-	33	38	-	
<b>Primary minerals:</b>																				
Olivine	Fo	44	34	47	44	26	35	25	38	32	24	48	41	23	42	34	-	26	-	33
Augite	Wo	33	34	31	35	34	33	32	34	27	-	31	32	-	31	30	37	29	33	35
	En	37	37	40	36	34	35	36	37	40	-	38	36	-	37	35	33	30	34	32
	Fs	20	18	19	17	21	21	21	18	24	-	14	18	-	16	21	19	24	18	18
	Jd	4	3	4	4	3	5	4	4	3	-	5	6	-	7	5	8	9	9	9
	Tsc	7	6	7	9	7	7	7	8	6	-	12	8	-	9	8	4	9	7	6
<b>Metamorphic minerals:</b>																				
Opx	En	-	-	-	-	54	51	-	52	46	63	57	43	57	52	50	46	51	52	51
	Fs	-	-	-	-	46	49	-	47	53	36	42	56	42	47	50	53	48	47	49
	(Wo)	-	-	-	-	(0.6)	(0.8)	-	(1.2)	(1.1)	(1.4)	(1.1)	(1.5)	(1.1)	(1.4)	(1.1)	(1.3)	(1.4)	(1.2)	(1.0)
Cpx	Wo	-	-	-	-	-	-	-	-	-	-	-	41	-	40	40	38	38	38	
	En	-	-	-	-	-	-	-	-	-	-	-	29	-	33	32	30	31	32	
	Fs	-	-	-	-	-	-	-	-	-	-	-	22	-	18	17	19	15	13	
	Jd	-	-	-	-	-	-	-	-	-	-	-	5	-	6	8	7	10	9	
	Tsc	-	-	-	-	-	-	-	-	-	-	-	4	-	4	4	4	6	7	
Garnet	Alm	-	-	-	-	-	-	-	-	-	-	-	-	63	63	65	61	61	64	
	Prp	-	-	-	-	-	-	-	-	-	-	-	-	16	17	13	17	17	17	
	Sps	-	-	-	-	-	-	-	-	-	-	-	-	3	2	3	2	2	2	
	Grs	-	-	-	-	-	-	-	-	-	-	-	-	19	19	19	19	20	17	
Spinel	Hc	-	-	-	-	-	-	-	-	-	-	-	-	-	71	74	71	73	-	
	Spl	-	-	-	-	-	-	-	-	-	-	-	-	-	19	18	21	21	-	
	Gah	-	-	-	-	-	-	-	-	-	-	-	-	-	4	2	3	2	-	
	Mag	-	-	-	-	-	-	-	-	-	-	-	-	-	6	6	6	4	-	

Normal, porphyritic and enriched diabase are identified by sample numbers T-, TP- and TE- respectively; samples are arranged in order from NW to SE across the Grenville Front (Fig. 2). Compositions reported for porphyritic dykes are of matrix minerals. Underlined sample numbers indicate those used for thermobarometric estimation. Mineral abbreviations after Kretz (1983), with addition of Tsc = Tschermak's molecule, Gah = gahnite.

Olivine is commonly completely replaced by a granular mosaic of orthopyroxene. The garnet-bearing symplectite is wider and lacks intergrowths of pyroxene along its outer edge; there, discrete, faceted grains of garnet project into the plagioclase. In some cases, clinopyroxene forms an ill-defined layer outboard of the orthopyroxene layer and is separated from the outermost garnet symplectite by a narrow layer (mm-scale) of oligoclase, corresponding to the "sodic plagioclase moat" described from other localities (*e.g.*, McLelland & Whitney 1980, Grant 1988, Johnson & Carlson 1990). Commonly, there is also a well-defined zone along the outer edge of the corona, where garnet interfingers symplectitically with K-feldspar (Fig. 6B), originally present along the margins of laths and in interstices. Garnet, however, is not present in the coronas around olivine enclosed in plagioclase xenocrysts; the two-fold orthopyroxene - (amphibole + spinel) coronas persist throughout Zone 4, where olivine has been largely or wholly consumed (Fig. 5D).

Coronas around oxide grains in Zone 4 maintain the same assemblage as in Zone 3, but are wider and coarser (Figs. 6C, 6D). The extent of recrystallization in plagioclase is variable; it is either limited along grain and twin boundaries, or encroaches into the

core of clouded laths, accompanied by coalescence of submicroscopic spinel as discrete grains (Fig. 4G). Augite show incipient recrystallization to fine, clear (ilmenite-free) secondary grains.

#### *Relationship of corona growth to deformation*

Shortening of the Sudbury dykes to give the folded forms evident in Figure 2 was accomplished by buckling and was accommodated internally by plastic distortion of primary minerals, most notably plagioclase, which is ubiquitously bent and kinked (Bethune 1997). Primary augite also shows evidence of plastic strain (deformation bands) in Zone 3, superseded in Zone 4 by subgrain development leading to recrystallization. The most important relationship, however, clearly seen in thin sections, occurs midway through Zone 3 and throughout Zone 4; the garnet symplectite rims common to oxide and matrix olivine coronas have overgrown deformed primary minerals, such as bent laths of plagioclase (Figs. 4D-G); the same is true in plagioclase xenocrysts, in which radiating amphibole-spinel symplectite has grown across curved twin lamellae. Both the coronas and plagioclase are in turn cut by later, more widely spaced

TABLE 2. COMPOSITIONS OF PRIMARY XENOCRYSTS AND RELATED METAMORPHIC FERROMAGNESIAN MINERALS IN PORPHYRITIC SUDBURY DIABASE AND METADIABASE

		Zone 1/2	-- Zone 3 --	--
Sample no.		TP-2	TP-3.1	TP-7
Mg# (rock)		40	-	41
<u>Primary minerals:</u>				
Olivine	Fo	71	66	55
Plagioclase core				
	An	57	59	58
	Ab	41	40	41
	Or	2	2	1
Plagioclase rim				
	An	33	30	48
	Ab	63	69	51
	Or	4	2	1
<u>Metamorphic minerals:</u>				
Opx	En	-	74	64
	Fs	-	26	35
	(Wo)	-	(0.6)	(1.2)
Pale green, low-Ti pargasite				
	Mg/Mg+Fe <sup>2+</sup>	-	-	0.83

fractures in Zone 3 and brittle-ductile shear zones in Zone 4. In the latter, minerals formerly in coronas are dispersed along the foliation and thoroughly recrystallized, resulting in a rock composed of thin, alternating layers and lenses with different proportions of extremely fine-grained (10–20 µm) orthopyroxene, clinopyroxene, garnet, biotite, plagioclase, spinel, ilmenite and apatite. The peak of corona development thus occurred at an intermediate stage in the overall history of deformation (Bethune 1998); there is thus clear evidence that the coronas formed during prograde metamorphism.

#### CHEMICAL COMPOSITION OF THE MINERALS

The compositions of the primary minerals in Sudbury diabase in Zone 1 serve as a reference in the evaluation of changes in their compositions as they become involved in corona-producing reactions. Compositional data for coexisting primary and metamorphic minerals in different types of diabase, arranged in order of occurrence in samples from northwest to southeast (Fig. 2), are presented in Tables

1 and 2 and are portrayed graphically in Figure 7. Mineral analyses were performed by energy-dispersion and wavelength-dispersion spectrometry on electron microprobes at Queen's University and the Geological Survey of Canada, respectively. The full set of analytical results (Bethune 1993) is available from the Depository of Unpublished Data, CISTI, National Research Council of Canada, Ottawa, Ontario K1A 0S2. An outline of analytical procedures, and the mineral compositions used specifically for thermobarometric calculations (see below), are provided in the Appendix.

#### Primary minerals

Single grains of *olivine* are slightly zoned with respect to Mg and Fe. Variation in composition by a few mol.% Fo among grains in a single sample may be an effect of random slices through similarly zoned grains. Nevertheless, there appears to be a real difference in composition between olivine in normal and Fe-enriched diabase. In normal diabase, olivine composition ranges from Fo<sub>47</sub> to Fo<sub>38</sub>, whereas in Fe-enriched diabase, it ranges from Fo<sub>35</sub> to Fo<sub>25</sub>; Mn content shows a strong positive correlation with the proportion of Fe. In porphyritic diabase, olivine inclusions in plagioclase xenocrysts have a much higher Fo content ( $\leq$ Fo<sub>70</sub>) than olivine in the matrix ( $\sim$ Fo<sub>40</sub>).

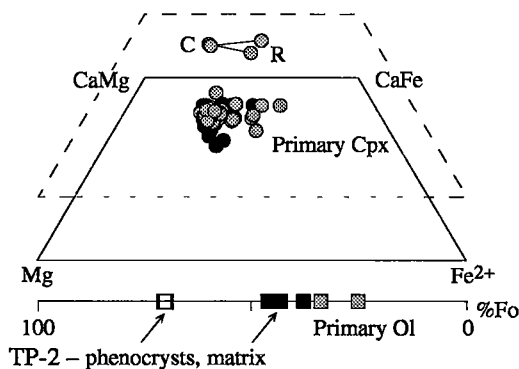
Large (2–3 mm), euhedral, violet or tan-colored grains of *titaniferous clinopyroxene* plot within the augite field (Fig. 7A). Grains are strongly zoned, with the core enriched in Ti, Mg and Al, and the rim depleted in these elements but enriched in Fe. The augite contains minor Na, corresponding to 3–4 mol.% of jadeite and aegirine components.

Zoned laths of *plagioclase* in normal diabase have a labradorite core (An<sub>60</sub>) that grades outward to andesine (An<sub>38</sub>) with an Or content of 2 to 3 mol.%. In Fe-enriched diabase, core-to-rim composition ranges from An<sub>54</sub> to An<sub>30</sub>, and the Or content is noticeably higher ( $\leq$ 6 mol.%). Where laths project into interstices, outer rims range to sodic oligoclase and may be succeeded by mesoperthite, grading to nonperthitic orthoclase. The rim of the laths is enriched in Ba relative to the core; the greatest concentration of Ba,  $\sim$ 3 mol.% celsian, is found in K-feldspar. The large, unzoned cores of plagioclase xenocrysts average An<sub>60</sub>, and their abrupt sodic overgrowths are in the range of sodic andesine (An<sub>30–40</sub>).

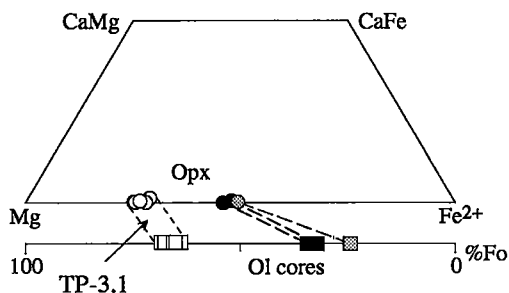
The Mg:Fe<sup>2+</sup> values of *biotite* indicate compositions midway between annite and phlogopite. The biotite normally contains between 3 and 5, and locally up to 6 wt. % TiO<sub>2</sub>, and hosts an appreciable concentration of Ba. F is more abundant than Cl; together, these anions comprise  $\sim$ 1 wt.%.

Opaque Fe–Ti oxides consist of blocky grains of finely exsolved magnetite–ulvöspinel with lamellae of ilmenite. Fine, blebby grains within magnetite–ulvöspinel are a solid solution between hercynite and

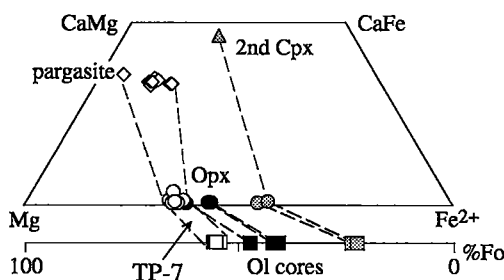
## A. ZONES 1 &amp; 2



## B. ZONE 2/3: GRENVILLE FRONT



## C. ZONE 3



## D. ZONE 4

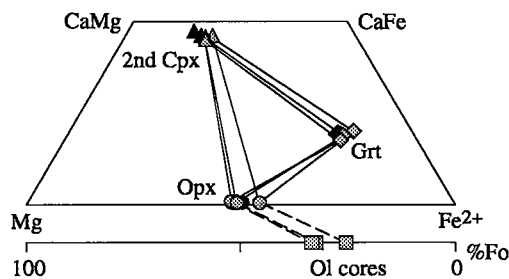


FIG. 7. Compositions of primary and secondary minerals in Sudbury diabase plotted in terms of Mg:Fe<sup>2+</sup> and Ca:Mg:Fe<sup>2+</sup> proportions (pyroxene quadrilateral) for successive zones across the Grenville Front. Black and grey symbols represent compositions of normal and Fe-enriched diabase, respectively. Open symbols represent compositions of coronas around olivine in porphyritic diabase. In A, core-rim pairs in primary augite are shown.

ulvöspinel. Ilmenite may also form thin lamellae within magnetite-ulvöspinel. No compositional data on oxide grains are presented.

#### Metamorphic minerals in coronas around olivine

In contrast to unreacted olivine in Zones 1 and 2, embayed olivine in the cores of coronas shows no evidence of chemical zoning. It is remarkably constant in composition in any one sample. Sample-to-sample variation in olivine from normal diabase ranges from Fo<sub>48</sub> to Fo<sub>42</sub>, and in Fe-enriched diabase, from Fo<sub>34</sub> to Fo<sub>23</sub>. The olivine forming the core of orthopyroxene-amphibole (spinel) coronas in two samples of porphyritic metadiabase in Zone 3 (TP-3.1, TP-7) is more magnesian (Fo<sub>66</sub> and Fo<sub>55</sub>, respectively). The Mg-number (Mg#) of olivine tends to decrease with increasing metamorphism relative to the Mg# of the

whole rock, reflecting preferential partitioning of Mg into the secondary minerals.

Orthopyroxene has a higher Mg# than olivine. Neglecting a minor wollastonite component ( $\leq 1.5$  mol.%), orthopyroxene in normal diabase ranges from En<sub>63</sub> to En<sub>50</sub>; that in Fe-enriched diabase ranges from En<sub>53</sub> to En<sub>44</sub>. Orthopyroxene compositions in the two samples of porphyritic metadiabase in Zone 3 are En<sub>74</sub> and En<sub>65</sub>, respectively.

Figure 8A illustrates changes in the Al and Ca content of orthopyroxene rims across the Grenville Front. Where they first occur, coincident with the Grenville Front mylonite zone, the average Al content ranges between 0.3 and 0.5 mol.%, and the Ca content between 0.3 and 0.4 mol.%. To the southeast, the Al content in orthopyroxene in Zones 3 and 4 is variable, but mainly greater than 1 mol.%, and the Ca content, relatively constant at about 0.5–0.7 mol.%. Within

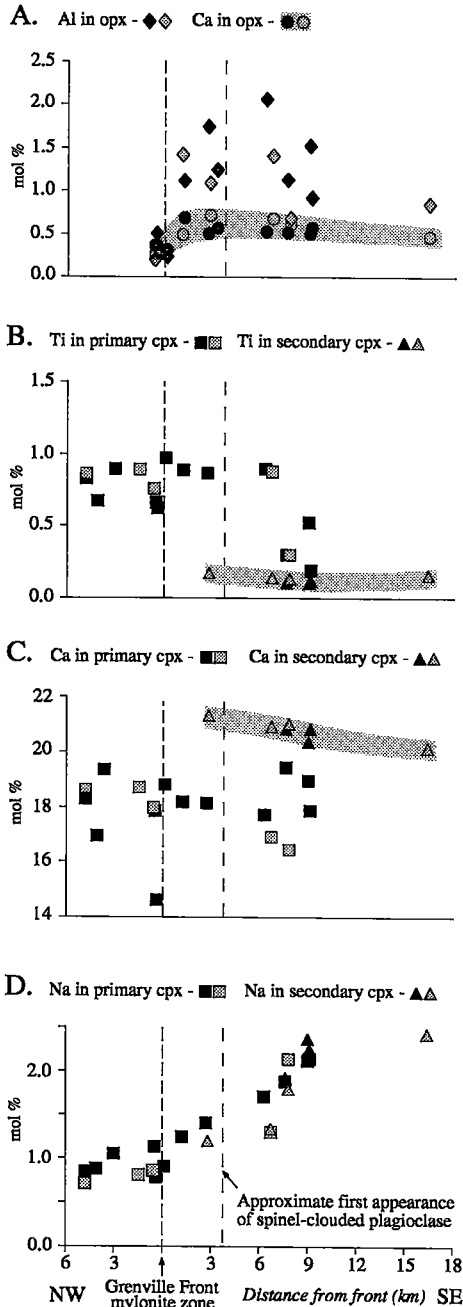


FIG. 8. Changes in mineral chemistry in Sudbury diabase across the Grenville Front. A. Changes in the Al and Ca content of metamorphic orthopyroxene. Shaded bar encompasses Ca values. B–D. Changes in composition of primary augite and secondary clinopyroxene; B: mol.% Ti, C: mol.% Ca, D: mol.% Na. Black symbols are normal diabase, grey are enriched diabase. In B and C, shading highlights compositional trends in secondary clinopyroxene.

individual coronas, the orthopyroxene layer shows a systematic outward increase in Al. Orthopyroxene inclusions within the garnet symplectite contain the most Al, typically 2–3 mol.%.

The composition of the secondary *clinopyroxene* overlaps with that of primary titaniferous augite (Fig. 7A), although there are significant differences between the two. The most noticeable of these is a markedly lower Ti content and a higher content of Na and Ca in the secondary clinopyroxene (Figs. 8B–D). The increase in Na is paralleled by a gradual increase in Al (after equating excess Ca with Al as Tschermak's component in the structural formula), resulting in an increase in the jadeite component. Compared with the zoned primary grains, the fine-grained metamorphic clinopyroxene also has a more uniform composition, particularly in terms of its Mg#; this is the case whether it is associated with olivine or oxide coronas or derived by recrystallization of primary grains.

It is noteworthy that, southeast of the front, the composition of clouded relict augite converges with that of coexisting secondary clinopyroxene (Figs. 8B–D). This is most obvious in terms of Na content, which in relict grains shows a steady increase southeastward from the front in parallel with secondary grains. The degree of convergence is more limited for Ca and Ti, probably reflecting their relatively lower mobility during metamorphism. The decrease in Ti content of relict grains can be directly attributed to the formation of the ilmenite lamellae.

The *pale green amphibole* forming the outer shell of olivine coronas in porphyritic diabase is an aluminous calcic amphibole in the compositional range pargasite – magnesiohastingsite (Leake *et al.* 1997); for simplicity, it is referred to henceforth as pargasite. In keeping with the higher Fo content of the reactant olivine, this amphibole has a somewhat higher Mg content than secondary clinopyroxene of either Fe-enriched or normal metadiabase (Figs. 7C, D). The  $K/(K + Na)$  value ( $\sim 0.36$ ) also is high relative to other reported compositions of amphibole in coronas of this type ( $\sim 0.07$ ; *e.g.*, Grieve & Gittins 1975, Mongkoltip & Ashworth 1983, Grant 1988), likely a manifestation of the generally high alkali content of Sudbury diabase. The green spinel intergrown with the amphibole is too fine to be analyzed; however, because both orthopyroxene and pargasite are more magnesian than the olivine that they surround (Table 2), it is probable that the spinel is relatively Fe-rich.

The average composition of *garnet* in normal diabase is  $Alm_{61}Prp_{18}Sp_{2}Grs_{19}$ , whereas that in Fe-enriched diabase is  $Alm_{64}Prp_{15}Sp_{3}Grs_{18}$ . Garnet composition varies little from one corona to another in the same rock, although in oxide coronas,  $X_{Alm}$  may be slightly higher than in olivine coronas;  $X_{Sp}$  generally varies proportionally with  $X_{Alm}$ . On the basis of stoichiometry, most garnet contains some  $Fe^{3+}$ , and hence a small amount of the andradite component.

The fine, green *spinel* formed upon recrystallization of clouded plagioclase is a solid solution between hercynite and spinel, with minor  $\text{Fe}^{3+}$  and Zn components ( $\text{Hc}_{71-74}\text{Spl}_{18-21}\text{Mag}_{4-6}\text{Gah}_{2-4}$ , from Table 1).

#### Metamorphic minerals in coronas around Fe–Ti oxide

The Fe–Ti oxide “cores”, like their counterparts northwest of the front, consist of ilmenite and magnetite–ulvöspinel, generally with ilmenite in excess of magnetite. Some exsolution lamellae of ulvöspinel are preserved in magnetite, but the lamellae are indistinct compared with examples from northwest of the front. In some cases, aluminous spinel occurs as lamellae or discrete grains within magnetite. This is characteristic of Broker metadiabase, where the spinel has a similar composition to hercynite exsolved

from plagioclase, but has a higher Mg# (e.g.,  $\text{Hc}_{60}\text{Spl}_{13}\text{Mag}_3\text{Gah}_2$  in T–9,  $\text{Hc}_{65}\text{Spl}_{12}\text{Mag}_4\text{Gah}_2$  in T–12).

Where metamorphic *biotite* first forms, coincident with the Grenville Front, it occurs as a very fine overgrowth on primary biotite and could not be analyzed separately. All biotite in Zone 3, whether primary or secondary, has a Ti content of 6 to >7 wt.%  $\text{TiO}_2$ . In Zone 4, the Ti content of biotite ranges between ~7.5 and 9 wt.%  $\text{TiO}_2$ , which is comparable to Ti abundances reported for biotite at other coronite localities (e.g., Whitney & McLelland 1983). Proportions of other elements do not vary in any detectable way from biotite northwest of the front.

Like the pale green pargasite around olivine typical of porphyritic diabase, the *olive-green amphibole* typical in oxide coronas also is aluminous. However, whereas the pale green pargasite has negligible Ti and more Mg than Fe, the olive-green amphibole has Ti values of ~0.4 atoms per formula unit (~40% kaersutite) and more Fe than Mg (Fig. 9). According to the classification of Leake *et al.* (1997), it is titanian and varies in composition from pargasite – ferropargasite to hastingsite. It generally has a higher K content [ $\text{K}/(\text{K} + \text{Na}) \sim 0.36$  to 0.48] than the pale green pargasite, particularly in the Fe-enriched metadiabase (Fig. 9). For purposes of comparison, it is referred to henceforth as titanian amphibole.

#### Change in plagioclase composition

The role of plagioclase in corona-forming reactions is well documented (Whitney & McLelland 1973, 1983, McLelland & Whitney 1980). As the reactions proceed, plagioclase becomes progressively enriched in the albite component as Ca diffuses outward from the core and is incorporated in metamorphic clinopyroxene and garnet. Excess Al in the plagioclase framework combines with incoming Mg and Fe to form aluminous spinel. Zoning profiles are gradually reduced as the composition of plagioclase becomes more uniformly sodic.

This progression is well illustrated in plagioclase of Sudbury diabase and metadiabase across the Grenville Front, where three stages of reaction have been distinguished (Fig. 10). Unreacted plagioclase in Zones 1 and 2 is characterized by regular zoning (Stage 1, Fig. 10A). In Zones 3 and 4, where spinel clouding has intensified, fairly steep zoning profiles are maintained (Stage 2, Fig. 10B). However, zoning is no longer evident in relict clouded cores once substantial recrystallization has taken place along grain margins (Stage 3, Fig. 10C). Recrystallized grains are depleted in the anorthite component relative to nearby relict cores, and are even more strongly depleted in An relative to cores of grains northwest of the front. The mean composition of recrystallized grains of normal diabase is  $\sim\text{An}_{30}$ , whereas that of Fe-enriched diabase is  $\sim\text{An}_{25}$ .

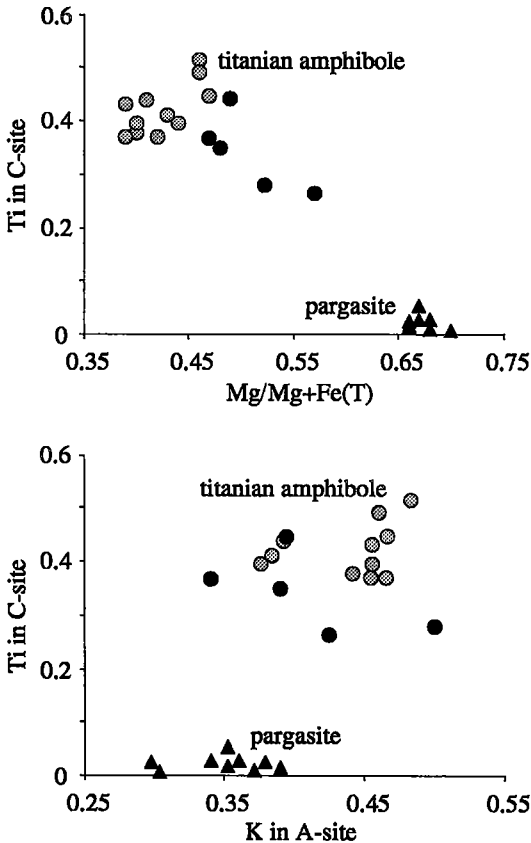


FIG. 9. Compositional differences between pale green amphibole (pargasite) in olivine coronas in porphyritic diabase and olive-green amphibole (titanian amphibole) in coronas around Fe–Ti oxide in nonporphyritic diabase. Black symbols represent normal diabase, grey symbols represent enriched diabase.

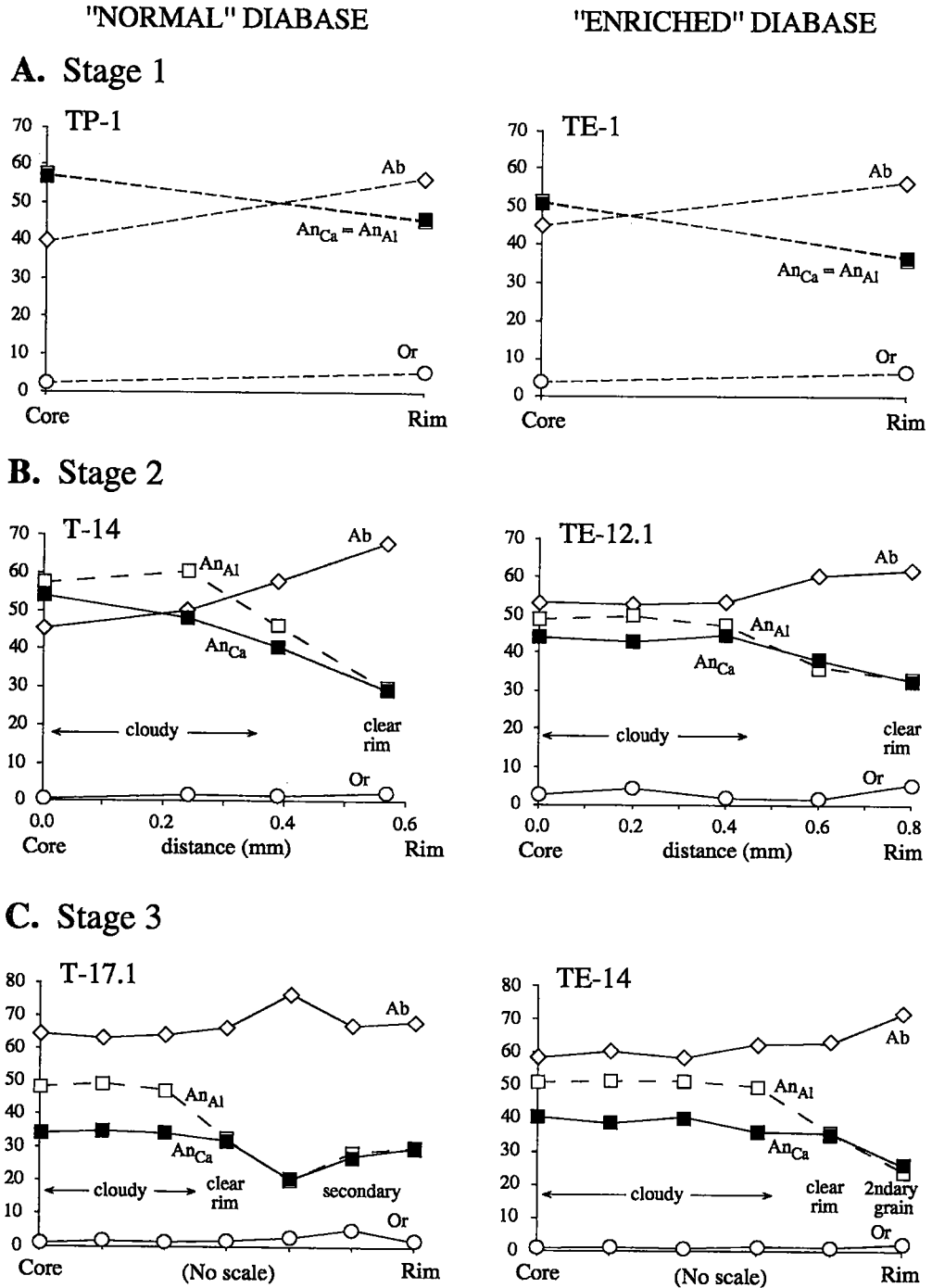


FIG. 10. Changes in plagioclase composition across the Grenville Front. A. Stage 1, typical core-to-rim zoning in laths of primary plagioclase in normal and Fe-enriched diabase, Zone 1. B. Stage 2, zoning profiles for unrecrystallized primary laths whose core is clouded by submicroscopic spinel, Zone 4. C. Stage 3, profiles across relict clouded cores that are mantled by recrystallized grains. The presence of spinel in former cores of labradorite in the primary plagioclase is indicated by the discrepancy between the An content calculated using the molar ratio  $Ca/(Ca+Na+K)$  ( $An_{Ca}$ ; black squares) and the ratio  $Al:Si$  ( $An_{Al}$ ; open squares). The zoning profiles shown by  $An_{Al}$  are assumed to reflect original compositions of igneous plagioclase.

Figure 10 illustrates how the contribution of Al from spinel has been monitored for each stage of reaction by comparing the calculated An content based on the atomic ratio:  $An_{Ca} = 100Ca/(Ca + Na + K)$ , with that based on the Al/Si ratio:  $An_{Al} = 100(3Al - Si)/(Al + Si)$ . In contrast to the clear rims, for which  $An_{Ca} \approx An_{Al}$ , cloudy cores all show  $An_{Ca} < An_{Al}$ . This discrepancy predictably increases from Stage 2 to 3, as clouding due to spinel intensifies and zoning diminishes. The Mg# of the clouded grains, about 0.2, also approximates the Mg# of the green spinel that has recrystallized from it. A more balanced feldspar composition is obtained for clouded grains by first removing a spinel component. The relationship between An content and presence or absence of clouding suggests that a threshold of  $\sim An_{3.5}$  was necessary for participation of plagioclase in spinel-forming reactions.

#### IDEALIZED REACTIONS

The identical whole-rock chemistry of metadiabase with respect to fresh Sudbury diabase northwest of the front suggests that metamorphism, although having involved significant transport of material by diffusion at grain scale, was isochemical with respect to the whole rock. Theoretically, it should thus be possible to account for the all metamorphic minerals without appealing to metasomatic introduction of material from outside the dykes. Two types of olivine corona have been described, namely around matrix olivine:

1a) orthopyroxene – clinopyroxene – garnet – spinel (in plagioclase),

and around olivine associated with plagioclase xenocrysts:

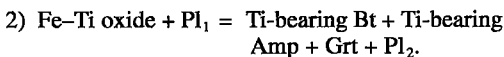
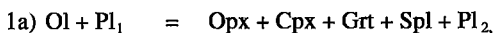
1b) orthopyroxene – pargasite–spinel symplectite.

Coronas around Fe–Ti oxide in all types of metadiabase consist of:

2) Ti-bearing biotite – Ti-bearing amphibole – garnet.

In both olivine and Fe–Ti oxide coronas, garnet is commonly symplectically intergrown with other product phases.

The following qualitative equations represent reactions producing the metamorphic mineral assemblages:



Balanced equations can be written for all of the above using mineral formulae that approximate closely their analyzed compositions (see Bethune 1993); the only additional elements required are the volatile components in biotite and amphibole ( $H_2O$ , F, Cl). In the reactions

represented by these equations, secondary plagioclase ( $Pl_2$ ) with a lower An content than reactant plagioclase ( $Pl_1$ ) is part of the metamorphic assemblage. The respective proportions of Mg and Fe in the different product phases are governed by two factors: 1) the original  $X_{Mg}$  of the olivine, and 2) the proportional amounts of olivine and Fe–Ti oxide that contribute to the final assemblage. Equation 2, as written, predicts no Mg component in the product phases, whereas analyses show appreciable Mg contents in biotite, amphibole and garnet. It is therefore necessary to invoke participation of olivine to provide the required Mg present in these phases.

The fact that the same reactant phases in equations 1a and 1b produce different assemblages under the same metamorphic conditions can be explained on the basis of the initial  $X_{Mg}$  of olivine, higher  $X_{Mg}$  values correlating with the production of pargasite + spinel (equation 1b) rather than garnet. Opx – (Prg + Spl) coronas similar to those found in plagioclase xenocrysts in Sudbury metadiabase have been reported in olivine gabbro with higher  $X_{Mg}$  (rock) values in which the primary olivine is much more magnesian than in the Sudbury diabase (e.g., Grieve & Gittins 1975, Rousell & Trevisiol 1988). Alternatively, isolation of olivine within plagioclase xenocrysts may have limited the participation of Fe–Ti oxide. In either case, it would seem that Prg + Spl symplectite is favored over garnet in Mg-rich starting materials under the same metamorphic conditions in which garnet forms in an Fe-rich environment. The fact that garnet symplectite first appears in Zone 3 in Fe-enriched dyke S-2' demonstrates that garnet formation is favored by Fe-rich bulk composition.

In summary, the assemblages of secondary minerals in coronas in Sudbury metadiabase can be produced using only the elemental components originally present in diabase. The volatile component required to produce amphibole and biotite is probably available from intergranular fluid or fluid inclusions present in the rock. In all of the above equations, conversion to proportionate volumes indicates that the product assemblages are denser than the reactant assemblages. This is in accord with measured differences in specific gravity of Sudbury diabase ( $\sim 3.0$ ) and metadiabase ( $\sim 3.15$ ), and is due principally to growth of garnet. Absence of garnet from coronas around olivine enclosed in plagioclase xenocrysts is explained by the more magnesian composition of this olivine, and the lack of access to iron from nearby oxide grains.

#### THERMOBAROMETRY

By their very nature, corona reaction textures indicate a state of chemical disequilibrium, and are therefore not ideal for estimation of metamorphic pressure and temperature. However, a number of studies on mechanisms of corona formation (e.g., Grant 1988)

have established that equilibrium conditions may be met at certain reaction interfaces, and that equilibrium may at least be achieved at a domainal scale. In Sudbury metadiabase, a good argument can be made that chemical potential gradients approached equilibrium on the basis that all secondary minerals, regardless of their textural setting (*e.g.*, in olivine or oxide coronas or in recrystallized domains) are remarkably uniform in composition.

P-T calculations were performed using the program TWEEQU (Thermobarometry with Estimation of Equilibration State) (Berman 1991), which computes all possible end-member equilibria for a given assemblage using an internally consistent thermodynamic database for minerals. For the present calculations, we used the version 2.02 database, which incorporates new standard state and mixing properties for clinopyroxene, orthopyroxene, olivine and garnet based on data systematics presented by Berman *et al.* (1995) and Berman & Aranovich (1996). The solid-solution model employed for plagioclase was that of Fuhrman & Lindsley (1988). For spinel, nonideal Fe-Mg interactions were derived (Berman, unpubl. data) from the experiments of Jamieson & Roeder (1984) on Fe-Mg partitioning between olivine and spinel.

The calculations were performed on five garnet-bearing samples, whose location are shown in Figure 2. Table 3 summarizes the P-T results for these samples and provides a key to the individual mineral compositions used in each calculation. Results of the analyses are reported in the Appendix, Tables A1 to A6. Three samples (TE-12.1, TE-14 and TE-15.1) are from the Fe-enriched dyke S-2'; all of these have fairly well-preserved coronas cored by olivine and Fe-Ti oxide. The two other samples (T-17.1, T-19) are from normal metadiabase. They contain coronas that are partly recrystallized and dispersed; olivine has been converted to orthopyroxene, and domains of recrystallized plagioclase contain abundant exsolved spinel. Sample T-17.1, from a late ductile shear zone, more closely approaches textural equilibrium than any of the other samples.

As well as calculating P, T and activity of components, TWEEQU enables an assessment of whether an assemblage has reached chemical equilibrium. Assuming that compositional and thermodynamic data are perfect, and activity models are appropriate for the minerals of interest, equilibrium is indicated when all equilibria converge to form a well-defined intersection in P-T space (Berman 1991). When all possible end-member equilibria were plotted for the Sudbury metadiabase assemblages, "convergence" was rarely obtained, even for the texturally best equilibrated sample T-17.1. In order to simplify interpretation, less reliable equilibria were thus discarded in favor of a smaller subset of independent reactions, chosen on the basis of being experimentally well calibrated and thermodynamically robust (least sensitive to errors in input).

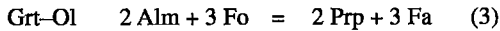
TABLE 3. SUMMARY OF P-T ESTIMATES IN SUDBURY METADIABASE

	Table no.							P (kbar)	T (°C)
	A2	A3	A4	A5	A6	A7			
	Ol	Opx	Cpx	Grt	Pl	Spl			
<b>TE-12.1</b>									
<i>Olivine corona</i>									
71-1a	1	1	1	1	1		6.6	730	
71-2a			2	2				740	
71-3a	1	2	3	3	1		6.8	740	
71-4a	1	3	4	4	1		6.3	710	
<i>Oxide corona 2a</i>									
71-5	1	4	5	5	2		7.4	750	
71-6			6	6				730	
71-7	1	5	7	7	2		7.0	730	
<i>Oxide corona 2b</i>									
71-9a	1	6	8	8	3		6.4	730	
71-10a	1	7	8	8	3		6.4	730	
71-11a			9	9				740	
71-12a			9	10				750	
<b>Average P and T</b>							<b>6.7</b>	<b>730</b>	
<b>TE-14</b>									
<i>Olivine corona</i>									
82-1	2	8	10	11	4		6.5	680	
82-2	2	9	10	11	4		6.5	690	
82-3	2	10	11	12	4		7.2	720	
82-4	2	10	11	13	4		7.5	740	
82-5			12	14				690	
82-6			12	15				720	
82-7			13	16				730	
82-8	2	11	11	13	4		7.5	740	
<i>Oxide corona</i>									
82-10			14	17				710	
82-11			14	18				710	
82-12			15	18				710	
82-13			15	19				750	
82-14			15	20				730	
82-16			16	21				750	
82-17			17	22				730	
<b>Average P and T</b>							<b>7.0</b>	<b>720</b>	
<b>TE-15.1</b>									
<i>Olivine corona</i>									
90-1a	3	12	18	23	5		8.4	730	
90-2a	3	13	19	23	5		8.3	730	
90-3a	3	14	20	24	5		9.0	750	
90-4a	3	15	21	25	5		7.9	700	
90-5a	3	12	18	26	5		8.5	740	
90-6a			22	27				780	
<b>Average P and T</b>							<b>8.4</b>	<b>740</b>	
<b>T-17.1</b>									
39-1		16	23	28	6	1	6.5	760	
<b>T-19</b>									
42-3		17	24	29	7	2	6.1	750	

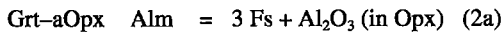
Numbers in left hand column represent individual microdomains, for which analyses (numbered) are reported in Tables A1 to A6 (appendix). P-T estimates are based on intersections of the Grt-Cpx thermometer and respective barometric equilibria. For microdomains containing only Grt and Cpx the temperature is quoted at the average pressure obtained for other microdomains. Values are rounded to the nearest tenth of a kilobar (pressure) and the nearest 10° Celsius (temperature). Realistic errors for P and T are  $\pm 1$  kbar and  $\pm 50^\circ\text{C}$ , respectively (Essene, 1989).

### Geothermometry

A number of solid-solid exchange equilibria are suitable for temperature calculations in the corona assemblages in Sudbury metadiabase. Among these are the Grt-Cpx, Grt-Opx, and Grt-Ol thermometers, based on the following reaction equilibria (in the following equations, note that the right side represents high temperature):



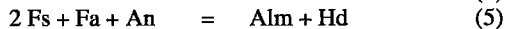
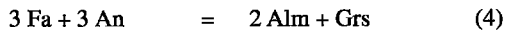
Of these, the exchange of Fe and Mg between Grt and Cpx is considered to be the most reliable, because it involves the largest equilibrium partitioning coefficient. The exchange reaction between Grt and Opx is the next most reliable thermometer; however, in granulite-facies assemblages, it commonly fails to retrieve peak temperatures, a phenomenon attributed to retrograde exchange of cations (Aranovich & Berman 1996, Pattison & Bégin 1994). In order to circumvent the effects of late Fe-Mg exchange, Aranovich & Berman (1996) recently developed a new Grt-Opx thermometer, based on the Al content of orthopyroxene, governed by the following net-transfer reaction:



### Geobarometry

Calculation of metamorphic pressure in Sudbury metadiabase is less straightforward since the standard barometric reactions for garnet-pyroxene granulites (e.g., Newton & Perkins 1982) involve quartz. In the absence of quartz, two approaches have been employed.

In *olivine-bearing samples*, in which olivine is still present in the core of coronas, the Grt-Cpx, Grt-Opx and Grt-Ol exchange thermometers (1-3) were computed in conjunction with two pressure-sensitive equilibria (eq. 4 and 5), as follows:

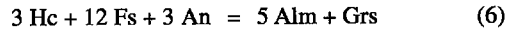


Reaction (4) has been calibrated experimentally by Bohlen *et al.* (1983) and has yielded geologically reasonable pressures in coronitic gabbros in the Adirondack Highlands (Johnson & Essene 1982) and the Central Gneiss Belt (Grant 1987), both in the Grenville Province.

For samples from dyke S-2', the full set of independent equilibria (1-5) was calculated for subsets of Opx-Cpx-Grt-(Ol-Pl) analyses in a number of microdomains across individual coronas. This methodology was used primarily to check whether or not certain microdomains showed signs of better equilibration than others, and also to test for general consistency in P-T values across, and between coronas. The composition of olivine for each subset is the same, as compositional variations across olivine cores were not detected. The composition of plagioclase, also constant for all subsets, represents that taken closest to the outer garnet symplectite rim. Where more than one analysis of plagioclase was made, these normally were found to differ slightly in composition (2-3 mol.% An),

and an average was used. In certain domains within the Grt-Px symplectite, orthopyroxene was not available for analysis, allowing only a temperature estimate (Grt-Cpx).

In *two-pyroxene - garnet granulites*, in which olivine has been fully consumed, the Grt-Cpx and Grt-Opx thermometers were computed together with two pressure-sensitive equilibria (eq. 6 and 7):



In these partly to fully recrystallized samples, mineral compositions were judged to be sufficiently homogeneous to warrant using average results of several analyses.

### Results

In the case of *olivine-bearing coronas along dyke S-2'*, P-T estimates for microdomains in each sample are listed in Table 3, and examples of data representing individual domains are plotted in Figures 11A-C. For each sample, all microdomains produced close agreement between the two barometric equilibria (eq. 4 and 5). In terms of temperature, the Grt-Cpx thermometer (1) yielded the most consistent results between microdomains, which in each case were generally in good agreement with the temperature resulting from the Grt-Ol thermometer (3). In contrast, the Grt-Opx thermometer (2) tended to define temperature on the order of 50 to >100°C lower than that of Grt-Cpx or Grt-Ol. This does not seem to reflect simple Fe-Mg resetting of orthopyroxene, on the basis that in most domains in most samples, the temperature given by the Grt-aOpx (2a) thermometer is similar to that defined by the standard Grt-Opx thermometer (2). Barring an unrecognized problem in calibration, a possible explanation is that the more resistant Al equilibrium preserves earlier conditions of orthopyroxene formation under conditions of lower temperature or higher pressure (or both), which is consistent with a clockwise P-T-t path for metamorphism of the Sudbury dykes (see below).

In view of the aforementioned relationships, plus the overall dependability of the Grt-Cpx thermometer relative to the others, the intersection between the Grt-Cpx thermometer and the two barometric equilibria is considered to be the most reliable estimate of pressure and temperature for these assemblages with relict olivine. In successive samples southeastward from the front (Table 3, Figs. 11A-C), this intersection occurs at progressively higher pressure but roughly the same temperature. For sample TE-12.1, located closest to the front (6.7 km), collective microdomain data define a pressure of 6.3 to 7 kbar and a temperature of 710 to 750°C. In sample TE-14, located ~1 km farther southeast, the P-T range encompassed by microdomains is 6.5 to 7.5 kbar and 680 to 750°C. For

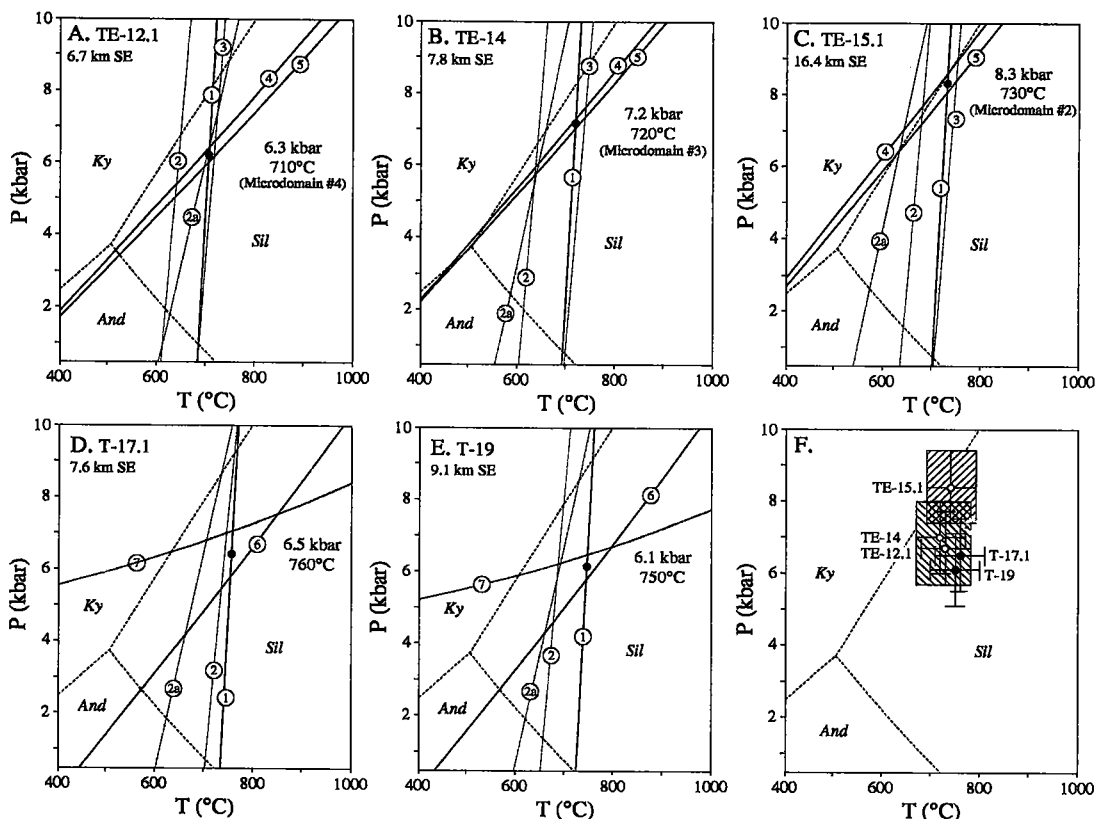


FIG. 11. P-T plots for Sudbury metadiabase; data from Table 3. A-C. Selected microdomains in olivine coronas in Fe-enriched metadiabase, dyke S-2' (A, 71-4a; B, 82-3; C, 90-2a). D, E. 2-Px-Grt-Spl assemblages from recrystallized coronas in normal metadiabase (D, 39-1; E, 42-3). F. P-T results for all samples, plotted with uncertainties ( $\pm 1$  kbar,  $\pm 50^\circ\text{C}$ ; Essene 1989). For relict olivine-bearing assemblages, values represent the average for all microdomains. Shaded rectangles highlight overlap in uncertainty ranges for dyke S-2' at ~8 and 16.4 km from the Grenville Front. Reaction equilibria were calculated with TWEEQU (Berman 1991), version 2.02 (BA96A.dat/sln), with the following activity-composition relationship: clinopyroxene: Berman *et al.* (1995); orthopyroxene, olivine and garnet: Berman & Aranovich (1996); plagioclase: Fuhrman & Lindsley (1988); spinel: Berman (unpubl. data).

sample TE-15.1, located farthest from the front (16.4 km), the data define a P-T range of between 7.9 and 8.5 kbar, and between 700 and 780°C.

In the case of *spinel-bearing samples*, P-T data are listed in Table 3 and portrayed graphically in Figures 11D and 11E. For consistency, P-T estimates are based on the intersection of the Grt-Cpx thermometer (1) and the two relevant barometers (eq. 6 and 7). In sample T-19, located 9 km from the front, this intersection occurs at 6.1 kbar and 750°C. Like the data for the olivine-bearing samples, the Grt-Opx (2) and Grt-aOpx (2a) thermometers overlap one another at a position down-temperature of the Grt-Cpx thermometer. In sample T-17.1, which is somewhat closer to the front (7.6 km), the same intersection occurs at 6.5 kbar and 750°C. In contrast to T-19, in which coronas are preserved, sample T-17.1 shows a greater degree of

textural equilibration, which may explain the closer agreement among various thermometers, particularly Grt-Cpx and Grt-Opx.

### Summary

A composite plot of the P-T data for all samples is shown Figure 11F. The maximum uncertainties assigned to each estimate are  $\pm 1$  kbar and  $\pm 50^\circ\text{C}$ , which are the generally accepted reliabilities of various published barometers and thermometers (Essene 1989). Collectively, the data indicate that rocks between ~7 and ~16 km of the Grenville Front mylonite zone were subjected to pressure in the range 5 to 9.4 kbar (16-30 km paleodepth) and temperature in the range 670° to 800°C during Grenvillian metamorphism. Despite evidence for textural disequilibrium, several

lines of evidence suggest that the results are meaningful:

(1) P–T estimates for the four samples ~8 km from the front lie within the stability field of sillimanite or just straddle the sillimanite–kyanite curve, compatible with the observation that sillimanite was the stable aluminosilicate in the host gneisses during Grenvillian metamorphism. The estimate for the fifth sample, TE–15.1, 16 km from the front, lies more substantially across the sillimanite–kyanite equilibrium curve; although kyanite was not observed near this sample site (the host rock is orthogneiss), it is present with sillimanite a few kilometers farther southeast (Corrigan *et al.* 1994).

(2) P–T estimates for the four samples approximately 8 km from the front, which represent both normal (T–17.1, T–19) and Fe-enriched (TE–12.1, TE–14) bulk compositions, all lie within the error limits ( $\pm 50^\circ\text{C}$ ,  $\pm 1$  kbar) for each sample. The P–T estimate obtained from the sample of sheared metadiabase (T–17.1) thus does not indicate markedly different conditions of equilibration from corona assemblages in less-deformed dykes.

(3) Considered alone, results from the three olivine-bearing samples along dyke S–2' show an increase in pressure with increasing distance from the front, at a relatively constant temperature of 730–740°C. The most substantial change in estimated pressure, from ~7 to 8.4 kbar, is between samples TE–14 (7.8 km) and TE–15.1 (16.4 km). Because the error limits for TE–15.1 overlap those of TE–12.1 and TE–14 combined (Fig. 11F), the significance of this apparent increase in pressure with distance from the front may be questioned. However, other physicochemical changes recorded in these rocks, such as the systematic increase in the Jd content (6 to 10 mol.%) in secondary clinopyroxene (Table 1), coupled with the noticeable decrease in the An content of plagioclase in the garnet-bearing samples (TE–14, TE–15.1, T–17.1, T–19; An<sub>26–21</sub>, Table A5), suggest that the rocks record a real southeastward increase in paleopressure. The trend to higher pressure (at comparable temperature) continues farther southeast, where peak conditions of 10–14 kbar and 650–800°C have been estimated from coronitic metadiabase southeast of the Boundary shear zone of the GFTZ (Jamieson *et al.* 1995).

(4) The estimated range in temperature (670°–800°C, including error limits) is within the range for structural distortion of plagioclase by dislocation creep (Tullis 1983, Tullis & Yund 1987, 1992; *cf.* Bethune 1997). It also is in accord with the closure temperature of minerals used for dating: at 8–10 km southeast of the front, titanite ( $T_c$  ~600°C; Heaman & Parrish 1991) has been significantly reset (Haggart *et al.* 1993), whereas monazite ( $T_c$  725  $\pm$  25°C; Parrish 1990) from metasedimentary gneiss close to metadiabase sample T–17.1 (Fig. 2) shows little or no Pb loss (Dudás *et al.* 1994). Lack of monazite resetting, however, suggests that temperature at this distance from the front did not

exceed 750°C, or that, if it did so, the duration of attainment of the peak temperature was too brief to instigate significant Pb loss from pre-Grenvillian monazite.

#### P–T HISTORY

By themselves, the P–T estimates from mineral assemblages in the coronas provide little information concerning the P–T trajectory followed by the rocks before final “quenching”. Despite the fact that some coronas may be produced in magmatic rocks during slow cooling following intrusion at depth, we consider that we have presented compelling evidence that the coronas in Sudbury metadiabase are a prograde metamorphic phenomenon, reflecting a substantial gradient in paleopressure and temperature across the Grenville Front. The geochronological data underpin this interpretation, indicating that more than 200 M.y. elapsed between dyke intrusion at ~1.24 Ga and growth of fine metamorphic zircon around primary baddeleyite, known to have begun by ~1.03 Ga. More direct evidence comes from the rocks themselves; for example, the fact that corona growth accompanied but outlasted plagioclase deformation, as indicated by textural relations preserved in metadiabase (Fig. 4), is compatible with a prograde (clockwise) P–T–t path. The coronas and deformed plagioclase are in turn deformed by younger, spaced microfaults, which vary from brittle in Zone 3 to ductile in Zone 4, where they are represented by the previously described shear-zones, in which all minerals are dynamically recrystallized. This sequence of microstructures agrees well with map-scale evidence for an evolution from early buckling of the dykes (reflecting compression orthogonal to the front) to later faulting and thrust–uplift concentrated along the front (Bethune 1998). Rather than representing discrete tectonic events, the two phases of dyke deformation may reflect early and late stages of continuous deformation separated by an interval of decreased strain that coincided with the thermal peak (Bethune 1997).

Although the P–T data from individual samples in this study are insufficient to define rigorous P–T–t paths, four of the five sample locations are at comparable distances from the Grenville Front, and textural relationships indicate that all samples shared a common metamorphic evolution, suggesting that it is unlikely that there are significant differences in P–T history between samples. Furthermore, assuming that P–T estimates at each site reflect conditions approaching  $T_{\text{max}}$ , it is reasonable to construct a hypothetical path comprising a family of similar paths for different structural levels, corresponding to different distances from the front. Such a path is shown in Figure 12; the tectono-metamorphic history of the Sudbury dykes is interpreted in terms of three major stages, defining a clockwise loop: (1) An early stage, characterized by

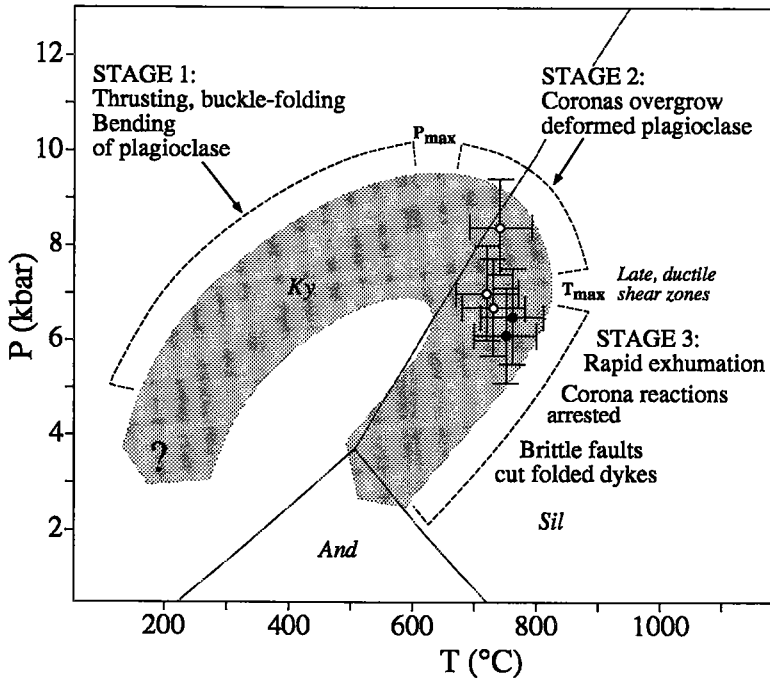


FIG. 12. Hypothetical P-T-t path for metamorphism of the Sudbury dykes. Shaded area represents potential family of P-T-t paths for metadiabase in Zones 3 and 4.

steadily increasing pressure and temperature, when dykes in the GFTZ were penetratively shortened by buckle folding and buried to a mid-crust level as a result of northwest-southeast compression and northwest-directed overthrusting. (2) An intermediate stage, during which coronas overgrew bent plagioclase. Local ductile shear zones, confined to the dykes, are interpreted as readjustment structures that formed more or less contemporaneously with  $T_{max}$ . Ignoring errors, it is notable that the highest temperature estimate was obtained from one of these zones (*i.e.*, 760°C in TE-17.1). (3) A stage of renewed compression and thrust exhumation, during which the dykes were deformed further as they were uplifted across the brittle-ductile transition. The resulting decrease in temperature is inferred to have been responsible for shutting down diffusion gradients, effectively "freezing in" corona textures. The youngest zones of mylonite and brittle faults, particularly those close to the Grenville Front, were preferentially localized along the pre-existing anisotropy between Zones 2 and 3 (*e.g.*, transition to southeast-dipping pre-Grenvillian gneisses), suitably oriented to accommodate further displacement. These structures clearly cut previously folded and metamorphosed dykes; they also cut and displace pre-Grenvillian isograds in the country rocks.

#### RELEVANCE TO REGIONAL TECTONIC MODELS

On the basis of regional structural, metamorphic and geochronological data in the GFTZ and northwestern Britt domain (*e.g.*, Haggart *et al.* 1993, Corrigan *et al.* 1994, Culshaw *et al.* 1994, Krogh 1994), Jamieson *et al.* (1995) proposed that thrusting in the northwestern part of the orogen in Ontario occurred in successive stages, one at  $\geq 1035$  Ma and the other at  $\geq 980$  Ma, separated by an interval of extension. This interpretation is based partly on principles of finite-element models (*e.g.*, Beaumont & Quinlan 1994, Beaumont *et al.* 1992, 1996), which predict that a crustal-scale, thrust-sense shear zone is created at the leading edge of a convergent orogen, and that, as convergence proceeds, the locus of shearing migrates toward the foreland. During the first stage ( $\geq 1035$  Ma), the limit of Grenvillian thrusting is considered to have been located along what is now the southeast margin of the GFTZ (Boundary shear zone in Fig. 1). During the second stage ( $\geq 980$  Ma), thrusting is interpreted to have migrated northwestward to what is now the Grenville Front, accounting for the somewhat younger ages of thermal activity in this area. Structural analysis indicates that during the intervening period, extension was restricted along and southeast of the Boundary

shear zone. Conflicting timing relations between compressional and extensional structures suggest that they occurred at virtually the same time (Jamieson *et al.* 1995), and the overall (*e.g.*, at orogen-scale) stress regime may have remained compressional (*cf.* Hodges *et al.* 1992). Extension is interpreted to have occurred at ~1020 Ma, the age of displacement along the Central Britt shear zone, a related extensional structure located ~60 km farther southeast (Ketchum *et al.* 1992, 1993, Culshaw *et al.* 1994). By relating P–T estimates to the geochronology and the succession of structural events established in this area, Jamieson *et al.* (1995) postulated a steep retrograde P–T–t path, reflecting rapid decompression.

The two stages of deformation recorded by the Sudbury dykes in the Tyson Lake area may well be a manifestation of the regional-scale thrusting events. In this matter, it is relevant that zircon in Sudbury metadiabase has two distinct morphologies and ages (Dudás *et al.* 1994). Fractions of coarser, anhedral zircon ( $\leq 50 \mu\text{m}$ ) are consistently older (1032–1024 Ma) than fine crystals of zircon ( $\leq 10 \mu\text{m}$ ) of aggregates that are direct pseudomorphs of baddeleyite (1008–988 Ma). The low U content of the anhedral zircon relative to baddeleyite in the same rock suggests that their older age is not related to an inherited isotopic component; they more likely represent a more advanced stage of baddeleyite replacement, as described by Davidson & van Breemen (1988). A plausible explanation for the spread in ages, given the evidence for only one period of metamorphism, is that both types of zircon grew as replacements of baddeleyite early in the metamorphic history (*e.g.*, some time before ~1030 Ma), but that the higher surface-areas of the finer grains allowed them to be progressively reset with continuing deformation to a limit of ~980 Ma, the time of final uplift (Bethune 1998; *cf.* Haggart *et al.* 1993). Bearing this in mind, we suggest that the first period of thrusting ( $\geq 1035$  Ma) proposed by Jamieson *et al.* (1995, Fig. 11) correlates with buckle folding and contemporaneous overthrusting of dykes in the GFTZ (Fig. 12, Stage 1), and that the second period, marked by renewed thrust propagation into the foreland ( $\geq 980$  Ma), correlates with further deformation (Fig. 12, Stage 3) as the dykes, previously buried by crust overthrust from the southeast, were uplifted along a relatively simple trajectory to higher levels in the crust. In the intervening period, the peak of dyke metamorphism (Fig. 12, Stage 2) is inferred to have coincided approximately with extensional activity in the interior of the orogen. This raises the possibility that decrease in strain rate required for growth of the delicate coronas may reflect the hypothesized interplay between compressional and extensional forces at this time.

This tectonic interpretation accounts for most of the features observed in the dykes, most notably the three-part tectono-metamorphic history documented in thin section (*e.g.*, plastic strain, maximum

development of coronas, superimposed deformation). An important implication is that the dykes were held at depth for as much as 20 M.y. between successive stages of deformation, during which the GFTZ was differentially buried (Jamieson *et al.* 1995). This is supported first-hand by mineral chemical and thermobarometric data indicating a southeastward increase in paleopressure to at least 8.5 kbar (~28 km depth) in the southeast part of the Tyson Lake area. Indirectly, it is also corroborated by the microscopic-scale strain history, which requires that a strong temperature-gradient was maintained across the front during the interval between pre- (Stage 1) and post-metamorphic (Stage 3) deformation (Bethune 1997). Note that, in the absence of intrusions of Grenvillian age, the heat for metamorphism can have only been supplied by an elevated geotherm related to thrusting (*cf.* Haggart *et al.* 1993). A point of further relevance is the abnormally high cooling-rate recorded in rocks close to the front (*i.e.*,  $14^\circ\text{C}/\text{M.y.}$ ; Haggart *et al.* 1993), indicating rapid late-stage uplift (at  $\geq 980$  Ma). The shutdown of diffusional processes at this time contributed to preservation of metamorphic coronas in the dykes. The late-stage uplift also resulted in telescoping of pre-Grenvillian isograds (~1.45 Ga) toward the front, now expressed by the fact that the metamorphic gradient in the host gneisses is steeper than in the dykes.

#### SUMMARY AND CONCLUSIONS

(1) Whole-rock geochemical data supported by geochronology indicate that olivine diabase dykes of the ~1.24-Ga Sudbury swarm in the Superior and Southern provinces cross the Grenville Front and are represented in the Grenville Province by deformed metadiabase dykes.

(2) The Sudbury dykes were emplaced across a previously established tectonic boundary and a metamorphic gradient that increases to the southeast, to which are related emplacement of granitic rocks at ~1.47 Ga, and subsequent deformation and regional metamorphism at ~1.45 Ga.

(3) Southeast of a line approximately coincident with this pre-existing front, the Sudbury dykes were deformed and progressively metamorphosed during Grenvillian orogeny at ~1.0 Ga, leading to development of classic coronite a few kilometers southeast of the front. The dykes are the only geological unit that records solely the effects of Grenvillian metamorphism; they also exhibit a metamorphic gradient less steep than that which had been formerly established in their country rocks.

(4) Textural relationships of minerals in metadiabase southeast of the Grenville Front, together with the chemical identity of Sudbury diabase and metadiabase, indicate that the metamorphic assemblages in the dykes formed by reaction of primary olivine and Fe–Ti oxide with plagioclase in a closed chemical

system. Balanced equations can be written to account for production of the observed metamorphic assemblages from these three primary minerals.

(5) Coronas of Opx – (Prg + Spl) around matrix olivine ( $FO_{<50}$ ) are spatially restricted to close to the front (Zone 2–3). In comparison, their occurrence around xenocrystic olivine ( $FO_{>65}$ ) in porphyritic metadiabase extends well into Zone 4; there, (Prg + Spl) around matrix olivine ( $FO_{<45}$ ) is absent in favor of Cpx–Grt. Incoming of garnet is promoted by more Fe-rich compositions, particularly where Fe–Ti oxide next to olivine has contributed Fe to form garnet, and olivine has contributed Mg for the silicates (titaniferous biotite, titaniferous amphibole and garnet). The contrasting distribution of different assemblages in the coronas across the Grenvillian metamorphic gradient attests to compositional control; caution must therefore be exercised in using corona assemblages as qualitative P–T indicators, especially where the compositions of primary reactant minerals may be variable.

(6) Textural and mineralogical changes in the dykes provide evidence for material transport by limited diffusion at grain scale to suitable sites of nucleation. Despite evidence for textural disequilibrium, the similarity in composition of secondary minerals throughout a given thin section indicates that equilibrium criteria were met locally. Thermobarometric calculations show that with careful choice of input parameters, complemented by knowledge of the regional metamorphic setting, meaningful P–T estimates can be obtained. Thermobarometry applied to mineral assemblages in the metamorphosed Sudbury dykes suggests that temperature between 670 and 800°C and pressure up to 8.5 kbar (~28 km paleodepth) were attained within 17 km of the front during Grenvillian metamorphism.

(7) The quantitative evidence for increasing paleopressure and temperature across the front, along with the progression of events indicated by mineral textural relationships in metadiabase, suggest a clockwise P–T–t path for metamorphism of the Sudbury dykes, consistent with regional models invoking progradation of the Grenvillian tectonic front toward its foreland.

#### ACKNOWLEDGEMENTS

This paper represents part of a Ph.D. study undertaken by the senior author at Queen's University, supervised by Drs. D.M. Carmichael and H. Helmstaedt. Financial and logistical support was provided by the Natural Sciences and Engineering Research Council and the Geological Survey of Canada. We thank Dr. P.L. Roeder and D. Kempson (Queen's University) and J. Stirling (Geological Survey of Canada) for assistance with electron-microprobe techniques, and Dr. R.G. Berman (Geological Survey of Canada) for help with interpretation of thermobarometric (TWEEQU) data. The paper benefitted from the constructive reviews of two anonymous referees.

#### REFERENCES

- ALBEE, A.L. & RAY, L. (1970): Correction factors for electron microprobe analysis of silicates, oxides, carbonates, phosphates and sulphates. *Anal. Chem.* **42**, 1408-1414.
- ARANOVICH, L.YA. & BERMAN, R.G. (1996): Optimized standard state and solution properties of minerals. II. Comparisons, predictions and applications. *Contrib. Mineral. Petrol.* **126**, 25-37.
- ASHWORTH, J.R. (1986): The role of magmatic reaction, diffusion and annealing in the evolution of coronitic microstructure in troctolitic gabbro from Risør, Norway: a discussion. *Mineral. Mag.* **50**, 469-473.
- BEAUMONT, C., KAMP, P.P.J., HAMILTON, J. & FULLSACK, P. (1996): The continental collision zone, South Island, New Zealand: comparison of geodynamical models and observations. *J. Geophys. Res.* **101**, 3333-3359.
- \_\_\_\_\_ & QUINLAN, G. (1994): A geodynamic framework for interpreting crustal-scale seismic-reflectivity patterns in compressional orogens. *Geophys. J. Int.* **116**, 754-783.
- \_\_\_\_\_, \_\_\_\_\_, HAMILTON, J. & WILLETT, S. (1992): Preliminary results from a mechanical model of the tectonics of compressive crustal deformation. In *Alberta Basement Transects, Workshop Report* (G.M. Ross, ed.). *Lithoprobe Rep.* **28**, 22-61.
- BERMAN, R.G. (1991): Thermobarometry using multi-equilibrium calculations: a new technique, with petrological applications. *Can. Mineral.* **29**, 833-855.
- \_\_\_\_\_ & ARANOVICH, L.YA. (1996): Optimized standard state and solution properties of minerals. I. Model calibration for olivine, orthopyroxene, cordierite, garnet and ilmenite in the system FeO–MgO–CaO–Al<sub>2</sub>O<sub>3</sub>–TiO<sub>2</sub>–SiO<sub>2</sub>. *Contrib. Mineral. Petrol.* **126**, 1-24.
- \_\_\_\_\_, \_\_\_\_\_ & PATTISON, D.R.M. (1995): Reassessment of the garnet – clinopyroxene Fe–Mg exchange thermometer. II. Thermodynamic analysis. *Contrib. Mineral. Petrol.* **119**, 30-42.
- BETHUNE, K.M. (1989): Deformation, metamorphism, diabase dykes, and the Grenville Front southwest of Sudbury, Ontario. *Geol. Surv. Can., Pap.* **89-1C**, 19-28.
- \_\_\_\_\_ (1993): *Evolution of the Grenville Front Southwest of Sudbury, Ontario with Emphasis on the Tectonic Significance of the Sudbury Diabase Dykes*. Ph.D. thesis, Queen's University, Kingston, Ontario.
- \_\_\_\_\_ (1997): The Sudbury dyke swarm and its bearing on the tectonic development of the Grenville Front, Canada. *Precambrian Res.* **85**, 117-146.
- \_\_\_\_\_ & DAVIDSON, A. (1988). Diabase dykes and the Grenville Front southwest of Sudbury, Ontario. *Geol. Surv. Can., Pap.* **88-1C**, 151-159.

- BICKFORD, M.E., VAN SCHMUS, W.R. & ZIETZ, I. (1986): Proterozoic history of the mid-continent region of North America. *Geology* **14**, 492-496.
- BOHLEN, S.R., WALL V.J. & BOETTCHER, A.L. (1983): Experimental investigation and application of garnet granulite equilibria. *Contrib. Mineral. Petrol.* **83**, 52-61.
- BROCOUM, S.J. & DALZIEL, I.W.D. (1974): The Sudbury basin, the Southern Province, the Grenville Front, and the Penokean orogeny. *Geol. Soc. Am., Bull.* **85**, 1571-1580.
- CARD, K.D. (1978): Geology of the Sudbury-Manitoulin area, Districts of Sudbury and Manitoulin. *Ont. Geol. Surv., Geol. Rep.* **166**; *Map 2360* (scale 1:126 720).
- \_\_\_\_\_ & LUMBERS, S.B. (1977): Sudbury-Cobalt. *Ont. Geol. Surv., Geol. Comp. Series, Map 2361* (scale 1:253440).
- CONDIE, K.C., BOBROW, D.J. & CARD, K.D. (1987): Geochemistry of Precambrian mafic dykes from the southern Superior Province of the Canadian Shield. In *Mafic Dyke Swarms* (H.C. Halls & W.F. Fahrig, eds.). *Geol. Assoc. Can., Spec. Pap.* **34**, 95-108.
- CORFU, F. & ANDREWS, A.J. (1986): A U-Pb age for mineralized Nipissing diabase, Gowganda, Ontario. *Can. J. Earth Sci.* **23**, 107-109.
- CORRIGAN, D., CULSHAW, N.G. & MORTENSEN, J.K. (1994): Pre-Grenvillian evolution and Grenvillian overprinting of the parautochthonous belt in Key Harbour, Ontario: U-Pb and field constraints. *Can. J. Earth Sci.* **31**, 583-596.
- CULSHAW, N.G., CORRIGAN, D., DRAGE, J. & WALLACE, P. (1988): Georgian Bay geological synthesis: Key Harbour to Dillon. *Geol. Surv. Can., Pap.* **88-1C**, 129-133.
- \_\_\_\_\_, DAVIDSON, A. & NADEAU, L. (1983): Structural subdivisions of the Grenville Province in the Parry Sound - Algonquin region, Ontario. *Geol. Surv. Can., Pap.* **83-1B**, 243-252.
- \_\_\_\_\_, KETCHUM, J.W.F., WODICKA, N. & WALLACE, P. (1994): Deep crustal extension following thrusting in the southwestern Grenville Province, Ontario. *Can. J. Earth Sci.* **31**, 160-175.
- DAVIDSON, A. (1990): Two transects across the Grenville Front, Killarney and Tyson Lake areas, Ontario. In *Exposed Cross-Sections of the Continental Crust* (M.H. Salisbury & D.M. Fountain, eds.). *NATO Adv. Study Inst., Ser. C* **317**, 343-400.
- \_\_\_\_\_ (1995): A review of the Grenville orogen in its North American type area. *Aust. Geol. Surv. Org., J. Aust. Geol. Geophys.* **16**, 3-24.
- \_\_\_\_\_ & BETHUNE, K.M. (1988): Geology of the north shore of Georgian Bay, Grenville Province of Ontario. *Geol. Surv. Can., Pap.* **88-1C**, 135-144.
- \_\_\_\_\_ & VAN BREEMEN, O. (1988): Baddeleyite - zircon relationships in coronitic metagabbro, Grenville Province, Ontario: implications for geochronology. *Contrib. Mineral. Petrol.* **100**, 291-299.
- \_\_\_\_\_ & \_\_\_\_\_ (1994): U-Pb ages of granites near the Grenville Front, Ontario. In *Radiogenic Age and Isotopic Studies, Rep. 8. Geol. Surv. Can., Pap.* **94-F**, 107-114.
- \_\_\_\_\_, \_\_\_\_\_ & SULLIVAN, R.W. (1992): Circa 1.75 Ga ages for plutonic rocks from the Southern Province and adjacent Grenville Province: what is the expression of the Penokean orogeny? In *Radiogenic Age and Isotopic Studies, Rep. 6. Geol. Surv. Can., Pap.* **92-2**, 107-118.
- DUDÁS, F.Ö., DAVIDSON, A. & BETHUNE, K.M. (1994): Age of the Sudbury diabase dykes and their metamorphism in the Grenville Province, Ontario. In *Radiogenic Age and Isotopic Studies, Rep. 8. Geol. Surv. Can., Pap.* **94-F**, 97-106.
- EMMETT, T.F. (1982): The petrography and geochemistry of corona-bearing dolerites from the Jotun Nappe, central southern Norway. *Mineral. Mag.* **46**, 43-48.
- ESSENE, E.J. (1989): The current status of thermobarometry in metamorphic rocks. In *Evolution of Metamorphic Belts* (J.S. Daly, R.A. Cliff & B.W.D. Yardley, eds.). *Geol. Soc., Spec. Publ.* **43**, 1-44.
- FAHRIG, W.F., GAUCHER, E.H. & LAROCHELLE, A. (1965): Paleomagnetism of diabase dykes of the Canadian Shield. *Can. J. Earth Sci.* **2**, 278-298.
- \_\_\_\_\_ & WEST, T.D. (1986): Diabase dyke swarms of the Canadian Shield. *Geol. Surv. Can., Map 1627A*.
- FRAREY, M.J. (1985): Proterozoic geology of the Lake Panache - Collins Inlet area. *Geol. Surv. Can., Pap.* **83-22**.
- FUHRMAN, M.L. & LINDSLEY, D.H. (1988): Ternary-feldspar modeling and thermometry. *Am. Mineral.* **73**, 201-215.
- GRANT, S.M. (1987): *The Petrology and Structural Relations of Metagabbros from the Western Grenville Province, Canada*. Ph.D. thesis, University of Leicester, Leicester, U.K.
- \_\_\_\_\_ (1988): Diffusion models for corona formation in metagabbros from the Western Grenville Province, Canada. *Contrib. Mineral. Petrol.* **98**, 49-63.
- GREEN, D.H. & RINGWOOD, A.E. (1967): An experimental investigation of the gabbro to eclogite transformation and its petrological applications. *Geochim. Cosmochim. Acta* **31**, 767-833.
- GRIEVE, R.A.F. & GITTINS, J. (1975): Composition and formation of coronas in the Hadlington gabbro, Canada. *Can. J. Earth Sci.* **12**, 289-299.
- GRIFFIN, W.L. (1971): Genesis of coronas in anorthositic of the Upper Jotun Nappe, Indre Sogn, Norway. *J. Petrol.* **12**, 219-243.
- \_\_\_\_\_ & HEIER, K.S. (1973): Petrological implications of some corona structures. *Lithos* **6**, 315-335.

- HAGGART, M.J., JAMIESON, R.A., REYNOLDS, P.H., KROGH, T.E., BEAUMONT, C. & CULSHAW, N.G. (1993): Last gasp of the Grenville orogeny: thermochronology of the Grenville Front Tectonic Zone near Killarney, Ontario. *J. Geol.* **101**, 575-589.
- HEAMAN, L. & PARRISH, R. (1991): Geochronology of accessory minerals. In Applications of Radiogenic Isotope Systems to Problems in Geology (L. Heaman & J.N. Ludden, eds.). *Mineral. Assoc. Can., Short-Course Handbook* **10**, 59-102.
- HODGES, K.V., PARRISH, R.R., HOUSH, T.B., LUX, D.R., BURCHFIELD, B.C., ROYDEN, L.H. & CHEN, Z. (1992): Simultaneous Miocene extension and shortening in the Himalayan orogen. *Science* **258**, 1466-1470.
- ITO, K. & KENNEDY, G.C. (1971): An experimental study of the basalt – garnet granulite – eclogite transition. In The Structure and Physical Properties of the Earth's Crust (J.G. Heacock, ed.). *Am. Geophys. Union, Monogr.* **14**, 303-314.
- JAMIESON, H.E. & ROEDER, P.L. (1984): The distribution of Mg and Fe<sup>2+</sup> between olivine and spinel at 1300°C. *Am. Mineral.* **69**, 283-291.
- JAMIESON, R.A., CULSHAW, N.G. & CORRIGAN, D. (1995): North-west propagation of the Grenville orogen: Grenvillian structure and metamorphism near Key Harbour, Georgian Bay, Ontario, Canada. *J. Metamorphic Geol.* **13**, 185-207.
- JOESTEN, R. (1986): The role of magmatic reaction, diffusion and annealing in the evolution of coronitic microstructure in troctolitic gabbro from Risør, Norway. *Mineral. Mag.* **50**, 441-467.
- JOHNSON, C.A. & ESSENE, E.J. (1982): The formation of garnet in olivine-bearing metagabbros from the Adirondacks. *Contrib. Mineral. Petrol.* **81**, 240-251.
- JOHNSON, C.D. & CARLSON, D. (1990): The origin of olivine – plagioclase coronas in metagabbros from the Adirondack Mountains, New York. *J. Metamorphic Geol.* **8**, 697-717.
- KAMO, S.L., KRÖGH, T.E. & KUMARAPATI, P.S. (1995): Age of the Grenville dyke swarm, Ontario – Quebec: implications for the timing of Iapetan rifting. *Can. J. Earth Sci.* **32**, 273-280.
- KETCHUM, J.W.F., CULSHAW, N.G. & JAMIESON, R.A. (1992): Structure, metamorphism and geochronology of high grade gneiss within and adjacent to the Central Britt shear zone, Central Gneiss Belt, southwest Grenville Province. *Geol. Assoc. Can. – Mineral. Assoc. Can., Program Abstr.* **17**, A57.
- \_\_\_\_\_, \_\_\_\_\_, KROGH, T.E. & JAMIESON, R.A. (1993): Late orogenic ductile extension on the middle Proterozoic Grenville orogen; an example from Ontario, Canada. In Late Orogenic Extension in Mountain Belts (M. Séranne & J. Malavieille, eds.). *Bureau de Recherches géologiques et minières (BRGM), Doc.* **219**, 108-109.
- KRETZ, R. (1983): Symbols for rock-forming minerals. *Am. Mineral.* **68**, 277-279.
- KROGH, T.E. (1994): Precise U–Pb ages for Grenvillian and pre-Grenvillian thrusting of Proterozoic and Archean metamorphic assemblages in the Grenville Front tectonic zone, Canada. *Tectonics* **13**, 963-982.
- \_\_\_\_\_, CORFU, F., DAVIS, D.W., DUNNING, G.R., HEAMAN, L.M., KAMO, S.L., MACHADO, N., GREENOUGH, J.D. & NAKAMURA, N. (1987): Precise U–Pb isotopic ages of diabase dykes and mafic to ultramafic rocks using trace amounts of baddeleyite and zircon. In Mafic Dyke Swarms (H.C. Halls & W.F. Fahrig, eds.). *Geol. Assoc. Can., Spec. Pap.* **34**, 147-152.
- \_\_\_\_\_, DAVIS, D.W. & CORFU, F. (1984): Precise U–Pb zircon and baddeleyite ages for the Sudbury area. In The Geology and Ore Deposits of the Sudbury Structure (E.G. Pye, A.J. Naldrett & P.E. Giblin, eds.). *Ont. Geol. Surv., Spec. Vol.* **1**, 431-446.
- \_\_\_\_\_, & DAVIS, G.L. (1970): Isotopic ages along the Grenville Front in Ontario. *Carnegie Inst. Wash., Yearbook* **68**, 309-313.
- KUSHIRO, I. & YODER, H.S., JR. (1966): Anorthite–forsterite and anorthite–enstatite reactions and their bearing on the basalt–eclogite transformation. *J. Petrol.* **7**, 337-362.
- LEAKE, B.E. and 21 others (1997): Nomenclature of amphiboles: report of the Subcommittee on Amphiboles of the International Mineralogical Association, Commission on New Minerals and Mineral Names. *Can. Mineral.* **35**, 219-246.
- LUMBERS, S.B. (1975): Geology of the Burwash area, Districts of Nipissing, Parry Sound and Sudbury. *Ont. Div. Mines, Geol. Rep.* **116**.
- \_\_\_\_\_, (1978): Geology of the Grenville Front Tectonic Zone in Ontario. In Toronto '78, Field Trips Guidebook (A.L. Currie & W.O. Mackasey, eds.). *Geol. Assoc. Can.*, 347-361.
- MCLELLAND, J.M. & WHITNEY, P.R. (1980): Compositional controls on spinel clouding and garnet formation in plagioclase of olivine metagabbros, Adirondack Mountains, New York. *Contrib. Mineral. Petrol.* **73**, 243-251.
- MONGKOLTIP, P. & ASHWORTH, J.R. (1983): Quantitative estimation of an open-system symplectite-forming reaction: restricted diffusion of Al and Si in coronas around olivine. *J. Petrol.* **24**, 635-661.
- MOORE, J.M. (1986): Introduction: the "Grenville Problem" then and now. In The Grenville Province (J.M. Moore, A. Davidson & A.J. Baer, eds.). *Geol. Assoc. Can., Spec. Pap.* **31**, 1-11.
- MØRK, M.B.E. (1986): Coronite and eclogite formation in olivine gabbro (western Norway): reaction paths and garnet zoning. *Mineral. Mag.* **50**, 417-426.

- NEWTON, R.C. & PERKINS, D., III (1982): Thermodynamic calibration of geobarometers based on the assemblages garnet – plagioclase – orthopyroxene – (clinopyroxene) – quartz. *Am. Mineral.* **67**, 203-222.
- NOBLE, S.R. & LIGHTFOOT, P.C. (1992): U–Pb baddeleyite ages of the Kerns and Triangle Mountain intrusions, Nipissing Diabase, Ontario. *Can. J. Earth Sci.* **29**, 1424-1429.
- PALMER, H.C., MERZ, B.A. & HAYATSU, A. (1977): The Sudbury dikes and the Grenville Front region: paleomagnetism, petrochemistry, and K–Ar ages. *Can. J. Earth Sci.* **14**, 1867-1887.
- PARRISH, R.R. (1990): U–Pb dating of monazite and its application to geological problems. *Can. J. Earth Sci.* **27**, 1431-1450.
- PATTISON, D.R.M. & BÉGIN, N.J. (1994): Zoning patterns in orthopyroxene and garnet in granulites: implications for geothermometry. *J. Metamorphic Geol.* **12**, 387-410.
- PEARCE, J.A. (1983): Role of sub-continental lithosphere in magma genesis at active continental margins. In *Continental Basalts and Mantle Xenoliths* (C.J. Hawkesworth & M.J. Norry, eds.). Shiva Press, Cheshire, U.K. (230-249).
- POUCHOU, J.L. & PICHOIR, F. (1984): A new model for quantitative X-ray microanalysis. *La Recherche aérospatiale* **3**, 167-192.
- RINGWOOD, A.E. & GREEN, D.H. (1966): An experimental investigation of the gabbro–eclogite transformation and some geophysical implications. *Tectonophys.* **3**, 383-427.
- RIVERS, T. & MENGEL, F.C. (1988): Contrasting assemblages and petrogenetic evolution of corona and noncorona gabbros in the Grenville Province of western Labrador. *Can. J. Earth Sci.* **25**, 1629-1648.
- ROUSELL, D.H. & TREVISIOL, D.D. (1988): Geology of the mineralized zone of the Wanapitei Complex, Grenville Front, Ontario. *Mineral. Deposita* **23**, 138-149.
- SHAND, S.J. (1945): Coronas and coronites. *Geol. Soc. Am., Bull.* **56**, 247-266.
- TUCKER, R.D., KROGH, T.E. & RÅHEIM, A. (1990): Proterozoic evolution and age-province boundaries in the central part of the Western Gneiss region, Norway: results of U–Pb dating of accessory minerals from Trondheimsfjord to Geiranger. In *Mid-Proterozoic Laurentia – Baltica* (C.F. Gower, T. Rivers & A.B. Ryan, eds.). *Geol. Assoc. Can., Spec. Pap.* **38**, 149-173.
- TULLIS, J. (1983): Deformation of feldspars. In *Feldspar Mineralogy* (P.H. Ribbe, ed.; second edition). *Rev. Mineral.* **2**, 297-323.
- \_\_\_\_\_ & YUND, R.A. (1987): Transition from cataclastic flow to dislocation creep of feldspar: mechanisms and microstructures. *Geology* **15**, 606-609.
- \_\_\_\_\_ & \_\_\_\_\_ (1992): The brittle–ductile transition in feldspar aggregates: an experimental study. In *Fault Mechanics and Transport Properties of Rocks* (B. Evans & Teng-Fong Wong, eds.). Academic Press, London, U.K. (89-117).
- VAN BREEMEN, O. & DAVIDSON, A. (1988): Northeast extension of Proterozoic terranes of mid-continental North America. *Geol. Soc. Am., Bull.* **100**, 630-638.
- WHITNEY, P.R. & MCLELLAND, J.M. (1973): Origin of coronas in metagabbros of the Adirondack Mountains, N.Y. *Contrib. Mineral. Petrol.* **39**, 81-98.
- \_\_\_\_\_ & \_\_\_\_\_ (1983): Origin of biotite – hornblende – garnet coronas between oxides and plagioclase in olivine metagabbros, Adirondack region, New York. *Contrib. Mineral. Petrol.* **82**, 34-41.
- WYNNE-EDWARDS, H.R. (1972): The Grenville Province. In *Variations in Tectonic Styles in Canada* (R.A. Price & R.J.W. Douglas, eds.). *Geol. Assoc. Can., Spec. Pap.* **11**, 263-334.

Received February 3, 1997, revised paper accepted July 11, 1997.

#### APPENDIX

##### *Analytical procedures*

At Queen's University, minerals were analyzed by energy-dispersion spectrometry using an ARL–SEMQ electron microprobe. Operating voltage was 15 keV, beam current, 100 nA, and counting times for each analysis, 100 s. Apparent concentrations between sample and standard were corrected for drift, dead time, background, and matrix effects using the technique of Bence and Albee (Albee & Ray 1970). A synthetic basaltic glass from the National Bureau of Standards (S–204) was used as the principal standard in

conjunction with a suite of secondary standards. At the Geological Survey of Canada, mineral analyses were performed by wavelength-dispersion spectrometry on a Cameca SX–150 electron microprobe using a range of standards for the elements of interest. Operating voltage was 15 keV. Counting times ranged between 20 and 30 seconds, with beam current between 10 and 30 nA. The data were reduced according to the procedure outlined in Pouchou & Pichoir (1984). A number of comparative tests were conducted (Bethune 1993), which indicated good agreement between compositions obtained on the same mineral grains on the respective microprobes.

## Analyses for thermobarometry

Mineral compositions obtained during this study (Bethune 1993) are filed with the Depository of Unpublished Data, CISTI, National Research Council of Canada, Ottawa, Ontario K1A 0S2. The following tables, A1 to A6, report only those compositions used in the calculation of metamorphic temperature and pressure (refer also to Table 3 in the text).

TABLE A1. CHEMICAL COMPOSITIONS OF OLIVINE USED FOR THERMOBAROMETRY

Sample no. Reference	TE-12.1		TE-14		TE-15.1	
	1	2	1	2	3	4
	av (8)	<i>lσ</i>	av (7)	<i>lσ</i>	av (7)	<i>lσ</i>
SiO <sub>2</sub>	32.97	0.20	31.54	0.21	32.89	0.23
TiO <sub>2</sub>	0.04	0.03	0.05	0.04	0.04	0.02
Al <sub>2</sub> O <sub>3</sub>	0.04	0.03	0.04	0.01	0.03	0.01
Cr <sub>2</sub> O <sub>3</sub>	0.03	0.03	0.01	0.01	0.03	0.02
FeO	52.04	0.64	56.44	0.83	53.00	0.28
MnO	0.52	0.05	0.48	0.07	0.33	0.05
NiO	0.07	0.05	0.03	0.02	0.04	0.05
MgO	14.78	0.23	11.02	0.08	14.43	0.08
CaO	0.04	0.03	0.12	0.04	0.04	0.04
Na <sub>2</sub> O	0.00	0.00	0.00	0.00	0.00	0.00
K <sub>2</sub> O	0.01	0.01	0.01	0.01	0.01	0.01
Σ	100.55		99.73		100.85	
Mol % end members						
Fo	33.3		25.6		32.5	
Fa	65.9		73.5		67.0	
Te	0.6		0.6		0.4	

TABLE A2. CHEMICAL COMPOSITIONS OF ORTHOPYROXENE USED FOR THERMOBAROMETRY

Sample no. Reference	TE-12.1						
	1	2	3	4	5	6	7
	071-4A2	071-4-2	071-4-1	071-2A	071-2B	071-2F	071-2E
Analysis							
SiO <sub>2</sub>	51.48	52.90	52.23	49.58	51.85	53.29	52.71
TiO <sub>2</sub>	0.05	0.07	0.05	0.17	0.03	0.06	0.07
Al <sub>2</sub> O <sub>3</sub>	1.14	0.76	1.34	0.83	1.04	0.78	1.52
Cr <sub>2</sub> O <sub>3</sub>	0.00	0.00	0.00	0.00	0.00	0.00	0.05
FeO	29.76	27.63	28.99	28.09	28.82	29.03	28.46
MnO	0.36	0.38	0.46	0.25	0.36	0.34	0.40
NiO	0.05	0.00	0.02	0.05	0.05	0.06	0.05
MgO	17.40	19.23	17.89	18.49	17.67	19.13	18.50
CaO	0.53	0.55	0.48	0.70	0.63	0.56	0.75
Na <sub>2</sub> O	0.00	0.00	0.00	0.00	0.00	0.00	0.00
K <sub>2</sub> O	0.00	0.04	0.01	0.01	0.00	0.01	0.02
Σ	100.77	101.56	101.46	98.17	100.45	103.26	102.53
Mol % end members							
En	50.7	54.8	51.9	55.8	51.5	53.8	52.8
Fs	48.27	44.1	47.2	42.7	47.2	45.1	45.6
Wo	1.1	1.1	1.0	1.5	1.3	1.1	1.5

TABLE A2 (CONTINUED)

Sample no. Reference	TE-14				TE-15.1				T-17.1	T-19	
	8	9	10	11	12	13	14	15	16	17	
	O82-12A5	O82-12A6	O82-12B	O82-12A2	O90-1C	O90-1A7	O90-1B	O90-1A6	av (4)	<i>lσ</i>	Opx 6a
Analysis											
SiO <sub>2</sub>	50.48	50.12	50.29	50.80	52.02	51.67	52.16	51.74	51.28	0.91	50.67
TiO <sub>2</sub>	0.09	0.06	0.11	0.05	0.04	0.1	0.08	0.08	0.12	0.19	0.11
Al <sub>2</sub> O <sub>3</sub>	0.52	0.64	0.67	0.65	0.71	0.73	0.72	0.81	1.02	0.51	1.2
Cr <sub>2</sub> O <sub>3</sub>	0.02	0.07	0.03	0.07	0.00	0.05	0.06	0.03	0.04	0.08	0.00
FeO	31.37	32.17	32.04	31.91	29.21	29.81	29.04	30.70	30.26	1.04	29.45
MnO	0.38	0.41	0.43	0.34	0.27	0.27	0.27	0.38	0.22	0.05	0.20
NiO	0.00	0.00	0.07	0.06	0.00	0.00	0.03	0.05			0.00
MgO	15.85	14.93	15.43	15.60	18.40	17.27	18.11	17.46	16.81	0.47	17.91
CaO	0.52	0.60	0.73	0.58	0.53	0.43	0.41	0.48	0.51	0.07	0.72
Na <sub>2</sub> O	0.00	0.00	0.00	0.00	0.00	0.00	0.00	0.00	0.03	0.05	0.00
K <sub>2</sub> O	0.02	0.01	0.00	0.01	0.01	0.00	0.00	0.00	0.16	0.26	0.00
Σ	99.25	99.01	99.81	100.05	101.21	100.32	100.88	101.75	100.56		100.26
Mol % end members											
En	47.1	44.7	46.0	46.1	53.0	50.3	52.2	50.6	49.5		52.8
Fs	51.8	54.0	52.4	52.7	45.9	48.8	47.0	48.4	49.5		45.7
Wo	1.1	1.3	1.6	1.2	1.1	0.9	0.9	1.0	1.1		1.5

TABLE A3. CHEMICAL COMPOSITIONS OF CLINOPYROXENE USED FOR THERMOBAROMETRY

Sample no.	TE-12.1										TE-14		
Reference	1	2	3	4	5	6	7	8	9	10	11	12	13
Analysis	C71-4A	C71-4E	C71-4-3	C71-4-2	C71-2B	C71-2A	C71-2C	C71-2D	C71-2E	C82-12B	C82-12E(1)	C82-12C	C82-12D
SiO <sub>2</sub>	52.24	50.08	52.72	52.78	52.93	52.64	53.53	53.50	53.00	51.93	51.01	51.54	51.86
TiO <sub>2</sub>	0.24	0.17	0.31	0.33	0.21	0.16	0.14	0.18	0.13	0.17	0.16	0.14	0.17
Al <sub>2</sub> O <sub>3</sub>	2.61	3.95	3.09	3.26	2.50	1.83	1.44	2.14	1.90	1.88	1.96	1.94	2.04
Cr <sub>2</sub> O <sub>3</sub>	0.00	0.00	0.00	0.05	0.06	0.00	0.01	0.00	0.00	0.00	0.00	0.04	0.01
FeO	12.13	12.87	12.57	11.84	12.68	11.84	11.99	12.32	12.15	13.08	14.48	13.29	13.41
MnO	0.27	0.45	0.20	0.24	0.24	0.24	0.18	0.22	0.20	0.18	0.25	0.20	0.19
NiO	0.00	0.05	0.10	0.00	0.05	0.00	0.00	0.00	0.00	0.02	0.00	0.04	0.03
MgO	11.67	11.47	11.53	11.74	11.93	11.86	12.08	12.04	11.92	11.10	10.42	10.76	10.51
CaO	20.81	18.65	21.41	21.58	20.76	21.00	21.74	21.17	21.72	20.92	20.73	20.87	20.89
Na <sub>2</sub> O	0.88	0.71	0.84	0.81	0.58	0.68	0.53	0.66	0.65	0.90	1.04	0.98	1.02
K <sub>2</sub> O	0.00	0.07	0.04	0.05	0.02	0.01	0.01	0.03	0.08	0.05	0.02	0.02	0.02
Σ	100.84	98.47	102.81	102.67	101.94	100.26	101.65	102.25	101.74	100.22	100.07	99.80	100.13
Mol % end members:													
En	32.4	32.8	31.6	32.0	33.0	33.2	33.4	33.1	32.9	31.2	29.4	30.4	29.7
Fs	17.4	19.4	17.2	16.7	19.9	18.6	18.9	19.1	17.3	17.8	17.6	17.8	18.8
Wo	39.3	34.2	39.1	39.4	39.4	41.3	42.6	40.6	41.3	40.3	39.0	40.2	40.5
Tsc	4.5	8.0	5.9	5.9	3.5	1.9	1.1	2.4	3.5	3.8	6.2	4.3	3.5
Jd+Ac	6.4	5.6	6.1	6.0	4.2	5.0	3.9	4.8	5.0	6.8	7.7	7.2	7.5

TABLE A3 (CONTINUED)

Sample no.	TE-14				TE-15.1					T-17.1	T-19
Reference	14	15	16	17	18	19	20	21	22	23	24
Analysis	C82-8A	C82-8B	C82-10I	C82-10J	90-1H	C90-1I	C90-1F	C90-1E	C90-1G	av (11) / σ	av (2)
SiO <sub>2</sub>	52.10	51.61	51.93	51.94	52.19	52.54	51.50	51.31	51.18	51.79	51.83
TiO <sub>2</sub>	0.15	0.16	0.26	0.14	0.22	0.24	0.24	0.25	0.25	0.17	0.09
Al <sub>2</sub> O <sub>3</sub>	1.84	2.05	2.05	1.97	2.84	2.61	2.93	2.98	2.76	2.27	2.27
Cr <sub>2</sub> O <sub>3</sub>	0.02	0.02	0.03	0.04	0.08	0.05	0.02	0.07	0.00	0.07	0.09
FeO	13.10	13.27	14.08	14.03	12.16	12.12	12.39	12.23	13.28	11.94	0.67
MnO	0.17	0.19	0.15	0.27	0.10	0.21	0.15	0.15	0.17	0.07	0.08
NiO	0.09	0.00	0.03	0.00	0.04	0.00	0.08	0.00	0.01	-	-
MgO	10.81	10.90	10.21	10.58	11.13	11.17	10.41	11.21	10.89	11.31	0.25
CaO	21.48	20.65	20.16	20.51	20.25	20.49	20.51	19.69	19.75	20.56	0.34
Na <sub>2</sub> O	0.95	0.98	1.09	0.96	1.41	1.31	1.20	1.29	1.15	1.06	0.13
K <sub>2</sub> O	0.02	0.03	0.01	0.05	0.01	0.04	0.01	0.01	0.04	0.03	0.05
Σ	100.73	99.86	100.00	100.48	100.42	100.79	99.44	99.17	99.48	99.43	100.65
Mol % end members:											
En	30.4	30.7	28.9	29.7	31.0	31.0	29.5	31.6	30.8	31.9	32.4
Fs	17.4	18.0	20.9	19.7	15.9	16.7	17.9	16.4	17.8	16.8	14.8
Wo	41.2	39.7	39.8	39.6	38.3	39.1	39.6	37.3	37.4	40.0	37.9
Tsc	4.0	4.3	2.3	3.7	4.4	3.5	4.1	5.1	5.3	3.5	5.7
Jd+Ac	7.0	7.3	8.1	7.3	10.3	9.6	8.8	9.5	8.6	7.9	9.2

TABLE A4. CHEMICAL COMPOSITIONS OF GARNET USED FOR THERMOBAROMETRY

Sample no.	TE-12.1										TE-14				
Reference	1	2	3	4	5	6	7	8	9	10	11	12	13	14	15
Analysis	T71-4A	T71-4A3	T71-4-3	T71-4-2	T71-2A3	T71-2A2	T71-2A4	T71-2B1	T71-2B2	T71-2B3	T82-12B	T82-12D	T82-12A	T82-12B1	T82-12B2
SiO <sub>2</sub>	37.38	38.12	38.63	38.65	38.89	38.62	38.75	39.17	39.01	39.19	37.42	37.72	37.50	37.36	37.27
TiO <sub>2</sub>	0.09	0.08	0.07	0.08	0.04	0.06	0.03	0.05	0.08	0.07	0.06	0.05	0.06	0.07	0.07
Al <sub>2</sub> O <sub>3</sub>	21.37	21.22	21.40	21.20	21.21	20.96	21.14	21.33	21.36	21.44	20.76	21.15	20.94	20.80	20.43
Cr <sub>2</sub> O <sub>3</sub>	0.00	0.00	0.04	0.09	0.00	0.00	0.04	0.00	0.00	0.03	0.00	0.03	0.00	0.01	0.00
FeO	29.41	29.81	29.42	29.70	29.54	29.36	29.93	30.45	29.54	29.22	31.21	31.25	31.00	30.97	28.86
MnO	1.41	1.34	1.58	1.48	1.09	1.02	1.14	1.19	1.07	1.15	1.27	1.24	1.26	1.41	1.23
NiO	0.00	0.00	0.10	0.00	0.00	0.00	0.03	0.00	0.00	0.10	0.06	0.01	0.00	0.10	0.00
MgO	4.38	4.30	4.03	3.99	4.30	4.25	4.17	4.38	4.22	4.37	3.24	3.06	3.37	3.13	2.94
CaO	6.28	6.34	7.16	7.16	6.39	6.63	6.42	6.30	7.18	7.03	6.81	7.03	6.80	6.93	7.82
Σ	100.32	101.19	102.32	102.35	101.45	100.90	101.61	102.88	102.45	102.49	100.77	101.53	100.92	100.67	98.63
Mol % end members															
And	63.0	63.5	62.1	62.5	63.7	63.2	64.0	64.1	62.4	61.9	66.4	66.5	66.0	66.1	63.6
Prp	16.7	16.3	15.1	15.0	16.5	16.3	15.9	16.4	15.9	16.5	12.3	11.6	12.8	11.9	11.6
Sps	3.1	2.9	3.4	3.2	2.4	2.2	2.5	2.5	2.3	2.5	2.7	2.7	2.7	3.0	2.7
Grs	17.2	17.3	19.4	19.3	17.6	18.3	17.6	17.0	19.4	19.1	18.6	19.2	18.5	19.0	22.1

TABLE A4 (CONTINUED)

Sample no.	TE-15.1										T-17.1		T-19	
Reference	16	17	18	19	20	21	22	23	24	25	26	27	28	29
Analysis	T82-12B5	T82-8C	T82-8D	T82-8E	T82-8F	T82-10D	T82-10E	T90-1F	T90-1B	T90-1A	T90-1H	T90-1C	av (4)	1σ
SiO <sub>2</sub>	38.18	37.60	37.78	37.79	37.20	37.56	37.59	38.07	38.25	38.03	37.86	38.29	38.36	0.48
TiO <sub>2</sub>	0.07	0.08	0.07	0.04	0.04	0.14	0.04	0.10	0.06	0.05	0.07	0.07	0.05	0.06
Al <sub>2</sub> O <sub>3</sub>	20.97	20.97	20.87	20.59	20.96	20.97	21.15	21.40	21.41	21.34	21.04	21.38	21.41	0.43
Cr <sub>2</sub> O <sub>3</sub>	0.00	0.03	0.00	0.00	0.00	0.04	0.03	0.02	0.03	0.06	0.09	0.00	0.00	0.00
FeO	29.51	30.82	30.93	30.00	30.06	30.12	30.31	30.05	29.94	30.78	30.04	29.37	28.62	0.35
MnO	1.18	1.11	1.10	1.13	1.26	1.23	1.29	1.03	0.97	1.05	0.93	1.00	0.74	0.13
NiO	0.11	0.00	0.01	0.05	0.00	0.04	0.07	0.07	0.01	0.00	0.01	0.02	-	-
MgO	3.30	3.33	3.45	3.77	3.49	3.38	3.26	4.14	4.12	3.98	4.24	4.33	4.27	0.16
CaO	6.72	6.72	6.86	6.61	6.77	6.57	6.79	6.45	6.35	6.29	6.18	6.26	6.88	0.52
Σ	99.93	100.65	101.05	99.94	99.79	99.99	100.46	101.26	101.13	101.58	100.46	100.70	100.34	100.67
Mol % end members														
And	65.3	66.3	65.8	64.8	65.0	65.8	65.7	64.3	64.5	65.5	64.7	63.7	62.5	61.7
Prp	13.0	12.8	13.1	14.5	13.5	13.1	12.6	15.8	15.8	15.1	16.3	16.7	16.6	17.1
Sps	2.6	2.4	2.4	2.5	2.8	2.7	2.8	2.2	2.1	2.3	2.0	2.2	1.6	2.1
Grs	19.1	18.5	18.7	18.3	18.8	18.4	18.9	17.7	17.5	17.1	17.0	17.4	19.3	19.0

TABLE A5. CHEMICAL COMPOSITIONS OF PLAGIOCLASE USED FOR THERMOBAROMETRY

Sample no.	1	2	3	4	5	6	7
Reference	P71-A,A1	P71-2A	P71-2A2,2A4	F82-12A1,3	P90-1A,A2	av (3)	(1)
Analysis							
SiO <sub>2</sub>	58.71	59.09	56.75	61.34	61.04	62.90	61.79
TiO <sub>2</sub>	0.02	0.00	0.02	-	0.07	0.00	0.09
Al <sub>2</sub> O <sub>3</sub>	24.73	24.91	25.89	23.88	22.71	22.95	23.55
Cr <sub>2</sub> O <sub>3</sub>	0.02	0.06	0.00	-	0.05	0.00	0.00
FeO	0.56	0.60	0.21	0.18	0.42	0.20	0.24
MnO	0.07	0.01	0.00	-	0.06	0.00	0.00
MgO	0.05	0.00	0.02	-	0.01	0.08	0.00
CaO	6.89	6.33	8.05	5.22	4.17	4.47	4.98
SiO	0.09	0.25	0.15	0.00	0.02	-	-
BaO	0.17	0.00	0.12	0.00	0.02	-	-
Na <sub>2</sub> O	7.59	8.00	7.02	8.66	9.33	8.86	8.68
K <sub>2</sub> O	0.25	0.20	0.19	0.13	0.51	0.33	0.39
Σ	99.13	99.46	98.39	99.38	98.38	99.79	99.72
Mol % end members							
An(Au)	33.7	34.4	39.9	26.3	22.1	20.8	24.5
Ab(Au)	64.7	64.5	58.9	73.0	75.2	77.3	73.4
Or(Au)	1.7	1.1	1.3	0.7	2.7	1.9	2.2
An(Ca+Sr)	33.0	30.5	38.5	24.8	19.3	21.4	23.5
Ab(Na)	65.3	68.4	60.2	74.5	77.9	76.7	74.3
Or(Ca-Ba)	1.7	1.1	1.3	0.7	2.8	1.9	2.2

TABLE A6. CHEMICAL COMPOSITIONS OF SPINEL USED FOR THERMOBAROMETRY

Sample no.	1	2
Reference	T-17.1	T-19
Analysis		
SiO <sub>2</sub>	av (9)	av (8)
TiO <sub>2</sub>	0.56	0.39
Al <sub>2</sub> O <sub>3</sub>	0.03	0.01
Cr <sub>2</sub> O <sub>3</sub>	55.90	57.10
FeO	0.03	0.00
MnO	37.32	35.36
NiO	0.00	0.14
MgO	0.05	0.12
ZnO	4.47	4.96
CaO	1.88	1.00
Σ	100.43	99.19
Fe <sub>2</sub> O <sub>3</sub> (calc)	5.58	3.76
FeO(calc)	32.30	31.97
Corr. wt. %	100.99	99.56
Mol % end members		
SpI	19.0	21.2
Hc	71.0	72.6
Gah	4.0	2.1
Mag	6.0	4.1